Arabidopsis ADR1 helper NLR immune receptors localize and function at the plasma membrane in a phospholipid dependent manner

Svenja C. Saile[1] (iD), Frank M. Ackermann[1], Sruthi Sunil[1] (iD), Jutta Keicher[1], Adam Bayless[2], Vera Bonardi[3], Li Wan[3], Mehdi Doumane[4], Eva Stöbbe[1], Yvon Jaillais[4] (iD), Marie-Cécile Caillaud[4] (iD), Jeffery L. Dangl[3,5] (iD), Marc T. Nishimura[2] (iD), Claudia Oecking[1] (iD) and Farid El Kasmi[1] (iD)

[1]Centre for Plant Molecular Biology (ZMBP), University of Tübingen, 72076 Tübingen, Germany; [2]Department of Biology, Colorado State University, Fort Collins, CO 80523-1878, USA; [3]Department of Biology, University of North Carolina, Chapel Hill, NC 27599, USA; [4]Laboratoire Reproduction et Développement des Plantes (RDP), Université de Lyon, ENS de Lyon, UCB Lyon 1, CNRS, INRAE, 69264, Lyon France; [5]Howard Hughes Medical Institute, University of North Carolina, Chapel Hill, NC 27599, USA

Summary

• Activation of nucleotide-binding leucine-rich repeat receptors (NLRs) results in immunity and a localized cell death. NLR cell death activity requires oligomerization and in some cases plasma membrane (PM) localization. The exact mechanisms underlying PM localization of NLRs lacking predicted transmembrane domains or recognizable lipidation motifs remain elusive.

• We used confocal microscopy, genetically encoded molecular tools and protein-lipid overlay assays to determine whether PM localization of members of the Arabidopsis HeLo-/RPW8-like domain 'helper' NLR (RNL) family is mediated by the interaction with negatively charged phospholipids of the PM.

• Our results show that PM localization and stability of some RNLs and one CC-type NLR (CNL) depend on the direct interaction with PM phospholipids. Depletion of phosphatidylinositol-4-phosphate from the PM led to a mis-localization of the analysed NLRs and consequently inhibited their cell death activity. We further demonstrate homo- and hetero-association of members of the RNL family. Our results provide new insights into the molecular mechanism of NLR localization and defines an important role of phospholipids for CNL and RNL PM localization and consequently, for their function.

• We propose that RNLs interact with anionic PM phospholipids and that RNL-mediated cell death and immune responses happen at the PM.

Introduction

Plant intracellular immune receptors of the nucleotide-binding leucine-rich repeat receptor (NLR) family mediate recognition of pathogen-derived effector proteins and the induction of a strong immune response. In many cases, NLR activation leads to the hypersensitive response (HR), a type of programmed cell death of the infected cells (Jones & Dangl, 2006; Monteiro & Nishimura, 2018; Balint-Kurti, 2019). Based on their N-terminal domain architecture, three classes of NLRs have been described in plants: Toll/Interleukin-1 receptor (TIR) NLRs (TNLs), coiled-coil (CC) NLRs (CNLs) and the HeLo/RPW8-like coiled-coil (CC$_R$) domain NLRs (RNLs) (Monteiro & Nishimura, 2018). In *Arabidopsis thaliana* (Arabidopsis) the RNL subclass consists of two gene families, *ACTIVATED DISEASE RESISTANCE 1* (*ADR1*) and *N REQUIREMENT GENE 1* (*NRG1*), both being required for immune signalling

and cell death induction of many other NLRs, particularly TNLs, and thus are also considered as 'helper' NLRs (Bonardi *et al.*, 2011; Qi *et al.*, 2018; Castel *et al.*, 2019; Lapin *et al.*, 2019; Wu *et al.*, 2019; Saile *et al.*, 2020). CNLs, TNLs and most likely RNLs might induce immune signalling and cell death by oligomerization (Wang *et al.*, 2019a; Hu *et al.*, 2020; Li *et al.*, 2020; Ma *et al.*, 2020; Martin *et al.*, 2020; Bi *et al.*, 2021; Jacob *et al.*, 2021; Wu *et al.*, 2021). CNL activation was speculated to result in the formation of a pore-like or membrane disrupting structure of the CC domains (a so-called resistosome) at the plasma membrane (PM) (Collier *et al.*, 2011; Burdett *et al.*, 2019; Wang *et al.*, 2019a; Xiong *et al.*, 2020; Bi *et al.*, 2021). Recently, it was demonstrated that the pentameric resistosome formed by CNL Arabidopsis HOPZ-ACTIVATED RESISTANCE 1 (AtZAR1) forms a cation-selective and calcium-permeable channel at the PM (Bi *et al.*, 2021). Calcium influx is known to trigger defence activation and cell death upon

NLR activation (Yoshioka *et al.*, 2006; Zhao *et al.*, 2021). PM localization is required for cell death and immune function of many CNLs, including Arabidopsis RESISTANCE TO PSEUDOMONAS SYRINGAE 5 (AtRPS5), RESISTANCE TO PSEUDOMONAS SYRINGAE PV MACULICOLA 1 (AtRPM1) and AtZAR1 (Gao *et al.*, 2011; Qi *et al.*, 2012; El Kasmi *et al.*, 2017; Wang *et al.*, 2019a, 2020a). By contrast, the subcellular localization of RNLs has not yet been analysed in detail. So far only the localization of AtNRG1s, but not of AtADR1s, was described. AtNRG1s were found to display a partial endoplasmic reticulum (ER) as well as a PM and cytosolic localization (Lapin *et al.*, 2019; Wu *et al.*, 2019; Jacob *et al.*, 2021). Remarkably, the autoactivated mutant AtNRG1.1^{DV} was observed to display an increased PM localization and additionally localized to puncta on the PM, suggesting that also RNLs function at the PM (Jacob *et al.*, 2021). The expression of activated AtNRG1.1^{DV} and AtADR1 resulted in an increase of the intracellular calcium concentration and further electrophysiological analysis revealed that RNLs can also act as potential PM-localized calcium-permeable channels (Jacob *et al.*, 2021), similar as shown for the CNL AtZAR1 (Bi *et al.*, 2021). Interestingly, many PM-localized CNLs and the RNLs have no predicted transmembrane domain/sequence or N- or C-terminal lipidation motifs and the mechanism that tethers them to the PM is unknown (Gao *et al.*, 2011). Thus, the molecular determinants driving their localization and cell death function at the membrane are not identified.

Homology modelling suggested that the CC$_R$ domains of RNLs share structural similarities with the N-terminal 4-helix bundle (HeLo domain) of mammalian MIXED-LINEAGE KINASE DOMAIN-LIKE (MLKL) proteins and fungal HET-s/ HELL proteins (Daskalov *et al.*, 2016; Bentham *et al.*, 2018; Jubic *et al.*, 2019). X-ray crystal structures of two mutant NRG1.1 CC$_R$ domains recently confirmed that AtNRG1.1 CC$_R$ resembles the MLKL 4-helix bundle (Jacob *et al.*, 2021). HeLo domains mediate the cell death function of MLKL and HET-s/ HELL proteins and are proposed to oligomerize and disrupt or permeabilize the PM (Hofmann, 2020; Murphy, 2020). PM localization and hence, cell death function of MLKL proteins requires the interaction of their HeLo domain with specific phospholipids at the PM (Dondelinger *et al.*, 2014; Quarato *et al.*, 2016).

Negatively charged phospholipids are low abundant lipids that mediate electrostatic interactions between membranes and proteins that contain polybasic or basic hydrophobic domains or clusters (McLaughlin & Murray, 2005; Heo *et al.*, 2006). Anionic phospholipids, including phosphatidylinositol phosphates (PIPs), phosphatidic acid (PA) and phosphatidylserine (PS), are particularly partitioned in membranes by type and thereby, contribute to organelle identity (Noack & Jaillais, 2017). The PM is the most electronegative compartment across eukaryotes (Yeung *et al.*, 2006; Simon *et al.*, 2016). In plants, phosphatidylinositol-4-phosphate (PI4P), PA and PS are required for the generation of the high electrostatic field of the PM (Simon *et al.*, 2016; Platre *et al.*, 2018). Especially, PI4P was found to be the main driver of the plant PM electronegativity (Simon *et al.*, 2016). While phosphatidylinositol 4,5

bisphosphate (PI(4,5)P$_2$) can also be found at the plant PM, it does not contribute to the PM surface charge (Simon *et al.*, 2016).

Expression of the PM-anchored catalytic domain of the yeast phospholipid-phosphatase Sac1p protein, which specifically dephosphorylates PM PI4P and therefore reduces PI4P levels and the PM electronegativity (Simon *et al.*, 2016; Gronnier *et al.*, 2017), can be used to determine whether a protein requires the presence of PI4P (or a high electronegativity) for localization and/or function at the PM. Depleting PI4P from the PM affects the localization and function of several proteins, including the auxin transport regulator PINOID or the BRASSINOSTEROID INSENSITITVE 1 (BRI1) kinase inhibitor 1 (BKI1) (Simon *et al.*, 2016).

We show that decreasing PI4P abundance at the PM results in the rapid degradation of the CNL AtRPM1 and the RNL family members AtADR1-L1 and AtADR1-L2. We also show that depleting PI4P from the PM causes a mis-localization of AtADR1 and the AtADR1s CC$_R$ domains. Mis-localized AtADR1 and AtADR1s CC$_R$ domains were severely impaired in their cell death activity, demonstrating that AtADR1s function at the PM.

Our results provide new insights into the molecular mechanism of NLR PM localization and defines an important role of the PM PI4P pool for the PM localization of AtRPM1 and AtADR1s. Further, our work indicates that AtADR1s deploy a lipid–protein interaction similar to mammalian MLKL proteins for PM localization, which is likely necessary for cell death execution at the PM. Our data also show that AtADR1s are capable of both homo- and hetero-association, suggesting that they form at least dimers or oligomeric complexes (resistosomes) for cell death induction.

Materials and Methods

Plasmid construction

Plasmid construction was done using standard techniques, including TOPO® cloning, GATEWAY™ cloning and Golden Gate cloning. Details are provided in Supporting Information Methods S1.

Transient expression in *Nicotiana benthamiana*

Agrobacterium tumefaciens overnight cultures were centrifuged and resuspended in induction buffer (10 mM MgCl$_2$, 10 mM MES pH 5.6, 150 µM acetosyringone). The optical density at 600 nm (OD$_{600}$) of all constructs was adjusted to 0.3 except of *35S::P19* which was adjusted to 0.05. Samples were mixed as indicated. Agrobacteria mixtures were infiltrated into leaves of 4 to 6-wk-old *N. benthamiana* wild-type (WT) plants. SAC1^{dead} and SAC1^{WT} as well as dOCRL^{dead} (*Drosophila melanogaster* orthologue of human oculocerebrorenal syndrome of *Lowe 1*) and dOCRL^{WT} co-infiltrations were always done on the same leaf to avoid expression differences that might arise from leaf-to-leaf variation. *Nicotiana benthamiana* plants were grown on soil under 12 h : 12 h, light : dark cycles (24°C : 22°C, 70% humidity). Induction of

protein expression was done 24 h post-infiltration by spraying using either 30 μM dexamethasone (Sigma-Aldrich, St Louis, MO, USA) and 0.001% (v/v) Silwet L-77 or 20 μM estradiol (Sigma-Aldrich) and 0.001% (v/v) Silwet L-77.

Chemical treatments

For protease inhibitor cocktail (PIC) and bortezomib (BTZ) treatments, *N. benthamiana* leaves were infiltrated with induction buffer only as Mock control or with induction buffer containing 2.5 μM BTZ (Santa Cruz Biotechnology, Dallas, TX, USA) or 1× Halt™ PIC (Thermo Fisher Scientific, Waltham, MA, USA) at 23 h post-Agrobacteria infiltration (hpi), For ADR1, 20 μM estradiol and 0.001% Silwet L-77 was infiltrated together with the Mock solution or the inhibitors to induce ADR1 expression. Leaf samples were collected 4 h (ADR1) or 5 h (ADR1-L1, ADR1-L2, RPM1) post-inhibitor/mock treatment.

Cell death assay

Indicated constructs were transiently expressed in *N. benthamiana* leaves and leaves were imaged for cell death as described in Methods S1.

Confocal imaging

Protein localization was analysed at the indicated time points with an inverse confocal laser scanning microscope LSM880 from Zeiss (Oberkochen, Germany) and an upright confocal laser scanning microscope TCS SP8 from Leica (Wetzlar, Germany) as described in Methods S1.

Western blot analysis of transiently expressed proteins

Frozen *N. benthamiana* leaf tissue was homogenized using a tissue homogenizer (Mill Retsch MM400; Retsch GmbH, Haan, Germany) and resuspended in grinding buffer (20 mM Tris-HCl pH 7, 150 mM NaCl, 1 mM EDTA pH 8, 1% (v/v) Triton X-100, 0.1% (w/v) SDS, 5 mM DTT, 1× Halt™ PIC (Thermo Fisher Scientific)). Samples were incubated on ice for 10 min and then centrifuged for 15 min at 16 000 g and 4°C. Then, 5× sodium dodecyl sulphate (SDS) loading buffer (250 mM Tris-HCl pH 6.8, 50% (v/v) glycerol, 500 mM DTT, 10% (w/v) SDS, 0.005% (w/v) bromophenol blue) was added to the supernatants, respectively. Proteins were denatured by incubation at 95°C for 5 min. SDS-PAGE (polyacrylamide gel electrophoresis), Western blotting and immunodetection followed standard procedures. Details for primary and secondary antibody dilutions are provided in Methods S1. Chemiluminescence was detected using an Amersham IMAGEQUANT 800 (GE Healthcare, Chalfont St Giles, UK). Images were processed with Adobe PHOTOSHOP CS2 (Adobe Inc., San José, CA, USA) for adjustment of brightness and contrast. Protein band intensities were determined by Western blot quantification using IMAGEJ as described by Hossein Davarinejad (http://www.yorku.ca/yisheng/Internal/Protocols/ImageJ.pdf). The quantification reflects the relative protein amounts as a ratio of the intensity of each protein band relative to the intensity of the lane's loading control (Rubisco band of the Ponceau stained membranes). Relative protein amounts were normalized to corresponding values from relative protein amounts of SAC1^{dead} or dOCRL^{dead} co-infiltrations, respectively.

Co-immunoprecipitation

Frozen *N. benthamiana* leaf tissue (*c.* 200 mg) was ground using liquid nitrogen and resuspended in 2.5 ml of extraction buffer (50 mM HEPES pH 7.5, 50 mM NaCl, 10 mM EDTA pH 8.0, 0.5% (v/v) Triton X-100, 5 mM DTT, 1× Halt™ PIC (Thermo Fisher Scientific)). Samples were kept for 20 min on ice and cleared by centrifugation at 16 000 g for 5 min and 16 000 g for 15 min at 4°C. Proteins were immunoprecipitated for 1 h using green fluorescent protein (GFP) Trap Beads (ChromoTek, Planegg-Martinsried, Germany). Further details are provided in Methods S1.

Microsomal fractionation

Microsomal membrane fractions were prepared from transgenic Arabidopsis plants expressing either *pADR1-L2::ADR1-L2-HA* or *pADR1-L2::ADR1-L2^{DV}-HA* (Roberts *et al.*, 2013). Plant tissue was ground in liquid nitrogen and sucrose buffer (20 mM Tris pH 8.0, 0.33 M sucrose, 1 mM EDTA, 5 mM DTT and 1× Halt™ PIC (Thermo Fisher Scientific)) was added in a ratio of 3 : 1. Samples were centrifuged at 2000 g for 10 min at 4°C to remove debris. Supernatants were transferred to fresh tubes and centrifuged again at 2000 g for 10 min at 4°C followed by an ultra-centrifugation step at 100 000 g for 45 min at 4°C. The microsomal pellet was resuspended in 50 μl sucrose buffer. 20 μg or 40 μg protein of each protein fraction (total, soluble, microsomes) was used for SDS-PAGE, respectively.

In vitro transcription and translation and PIP strip assay

ADR1 CC$_R$-HA (1–146 aa), ADR1-L1 CC$_R$-HA (1–155 aa), ADR1-L2 CC$_R$-HA (1–153 aa), RPM1 CC-HA (1–156 aa) and Citrine-HA were expressed *in vitro* using the TnT® SP6 High-Yield Wheat Germ Protein Expression System (Promega, Madison, WI, USA) according to the manufacturer's instructions. A PCR-generated DNA fragment was used as template for the transcription and translation reaction. Primers are listed in Table S1. Protein synthesis was confirmed on Western blot using an haemagglutinin (HA)-specific antibody. Lipid overlay assays using PIP strips were performed according to the manufacturer's instructions (Echelon Biosciences, Salt Lake City, UT, USA) and as described in Reuter *et al.* (2021).

Transmembrane, lipidation and membrane binding sites predictions

Predictions for transmembrane domains, lipidation motifs and membrane binding sites were done using different online tools as described in Methods S1.

Results

AtADR1s localize to the plasma membrane in *N. benthamiana*

The subcellular localization of two Arabidopsis full length RNLs, AtNRG1.1 and AtNRG1.2, was recently described. Both proteins localize to ER membranes, partially to the PM and in the cytosol when transiently expressed in *N. benthamiana* and analysed by confocal microscopy or subcellular fractionation experiments (Lapin *et al.*, 2019; Wu *et al.*, 2019; Jacob *et al.*, 2021). Their intracellular localization was not changed upon effector-triggered and TNL-mediated activation (Qi *et al.*, 2018; Wu *et al.*, 2019). However, the autoactivated mutant of AtNRG1.1 displayed increased PM localization and additionally, localized in puncta on or close to the PM (Jacob *et al.*, 2021). Information on the localization of the other RNL subfamily, the AtADR1s, is missing. To investigate the subcellular localization of the three AtADR1 proteins pre- and post-activation, we transiently expressed C-terminally EYFP- or Citrine-HA-tagged WT AtADR1, AtADR1-L1 and AtADR1-L2 in *N. benthamiana* leaves under the control of an estradiol inducible or 35s promotor (Figs 1a,d,g, S1a,c,e,g) and their native promotors (Fig. S2a–c). We observed no difference in the localization pattern of the AtADR1 proteins, regardless of the promotor used (Figs 1a,d,g, S1a,c,e,g, S2a–c). All three AtADR1 WT proteins co-localized with the PM-localized receptor-like kinase BRI1-mRFP (Figs 1a, d,g, S1a,e,g, S2a–c) (Friedrichsen *et al.*, 2000). In contrast to AtADR1-L1 and AtADR1-L2 the localization of AtADR1 was not restricted to the PM. AtADR1 additionally localized to (1) the ER membrane, since we observed a co-localization with the ER-resident plant V-ATPase assembly factor AtVMA12-RFP (Fig. S1c) (Viotti *et al.*, 2013) and to (2) puncta, some of which might be PM and/or ER associated (Fig. S1a,c).

In order to confirm the membrane association of AtADR1s in Arabidopsis, we performed subcellular fractionation experiments of protein extracts prepared from Arabidopsis seedlings stably expressing AtADR1-L2-HA under control of its native promoter. AtADR1-L2-HA was clearly enriched in the microsomal membrane fraction compared to the soluble fraction, demonstrating that also in Arabidopsis, AtADR1-L2 is mainly associated with membranes (Fig. S2d). These results suggest that AtADR1 proteins might display a similar localization pattern in Arabidopsis as observed in *N. benthamiana* and hence, might also primarily be PM localized.

Since NLR localization might change once the receptor is activated (Wang *et al.*, 2019a; Jacob *et al.*, 2021), we generated autoactive versions of AtADR1s by mutating a conserved aspartic acid in the MHD motif to valine, referred to as DV (QHD to QHV in AtRNLs; cell death phenotype of autoactivated AtRNLs shown in Figs 2a, S3) (Van Ooijen *et al.*, 2008; Williams *et al.*, 2011; Roberts *et al.*, 2013). We also generated AtADR1 P-loop mutants (GKT to AAA), referred to as AAA, to determine whether loss of P-loop function, which was shown to affect the canonical function of at least AtADR1-L2 (Roberts *et al.*, 2013), has an effect on AtADR1s localization. Confocal microscopy

analyses revealed that all three AtADR1 P-loop mutant proteins still localized to the PM, but also in the cytosol and/or to the ER (Fig. 1b,e,h), similar as observed previously for AtNRG1.1 loss of cell death function mutants (Jacob *et al.*, 2021). By contrast, autoactivated AtADR1 proteins strongly resembled the localization of AtADR1 WT proteins and thus, were found to be localized to the PM (AtADR1^{DV}, AtADR1-L1^{DV}, AtADR1-L2^{DV}) and ER (ADR1^{DV}) (Figs 1c,f,i, S1b,d,f,h). We also noticed that AtADR1^{DV} and AtADR1-L1^{DV} localized to BRI1-mRFP positive puncta (Figs 1c,f, S1b,f), most likely endosomes and/or PM nanodomains. This however was not observed for AtADR1-L2^{DV} (Figs 1i, S1h).

We performed subcellular fractionation experiments using protein extracts prepared from transgenic Arabidopsis plants expressing the auto-activated mutant AtADR1-L2^{DV}-HA under control of its endogenous promoter to validate the membrane association of activated AtADR1s in Arabidopsis. AtADR1-L2^{DV}-HA was enriched in the microsomal membrane fraction compared to the soluble fraction, confirming that also in Arabidopsis, AtADR1-L2^{DV} primarily is associated with membranes (Fig. S2e).

These results demonstrate that the three members of the AtADR1 subfamily localize to the plant PM pre- and post-activation and further suggest that AtADR1 WT (steady-state) additionally localizes to ER membranes and ER-associated dot-like structures, as observed for AtNRG1.1 (Lapin *et al.*, 2019; Wu *et al.*, 2019; Jacob *et al.*, 2021). Given the high similarity (70–75%) of the protein sequence between the AtADR1 family members, the additional ER localization of AtADR1 was unexpected. We speculate that differences in interaction partners of the three AtADR1s are likely causal for this localization. However, the PM localization of all (auto-)activated AtADR1s suggests that they also execute their immune (cell death) function at the PM.

Homo- and hetero-association of AtADR1s

NLR function in plants and animals is proposed to require oligomerization for proper induction of cell death and immunity (Wang & Chai, 2020). Recently, it has been shown that autoactive AtNRG1.1^{DV} forms high molecular weight complexes, whereas inactive mutant AtNRG1.1 variants did not (Jacob *et al.*, 2021). If the formation of the high molecular weight complexes of AtNRG1.1^{DV} involves homo-oligomerization is not known, but very likely, given that *N. benthamiana* NRG1 self-associates (Qi *et al.*, 2018). Likewise, AtADR1-L1 was found to self-associate and this self-association was enhanced upon immune activation (Wu *et al.*, 2021). On that basis, we tested, whether all three AtADR1 proteins are capable of forming homo- and also hetero-dimers and whether these associations are dependent on their activation status. First, we analysed the capability of AtADR1 WT and the autoactivated QHV mutant (DV) proteins to induce a cell death response after transient over-expression in *N. benthamiana*. We observed that over-expression of AtADR1, AtADR1^{DV} and AtADR1-L1^{DV} induced a HR-like cell death, whereas the over-expression of ADR1-L2^{DV} only resulted in a
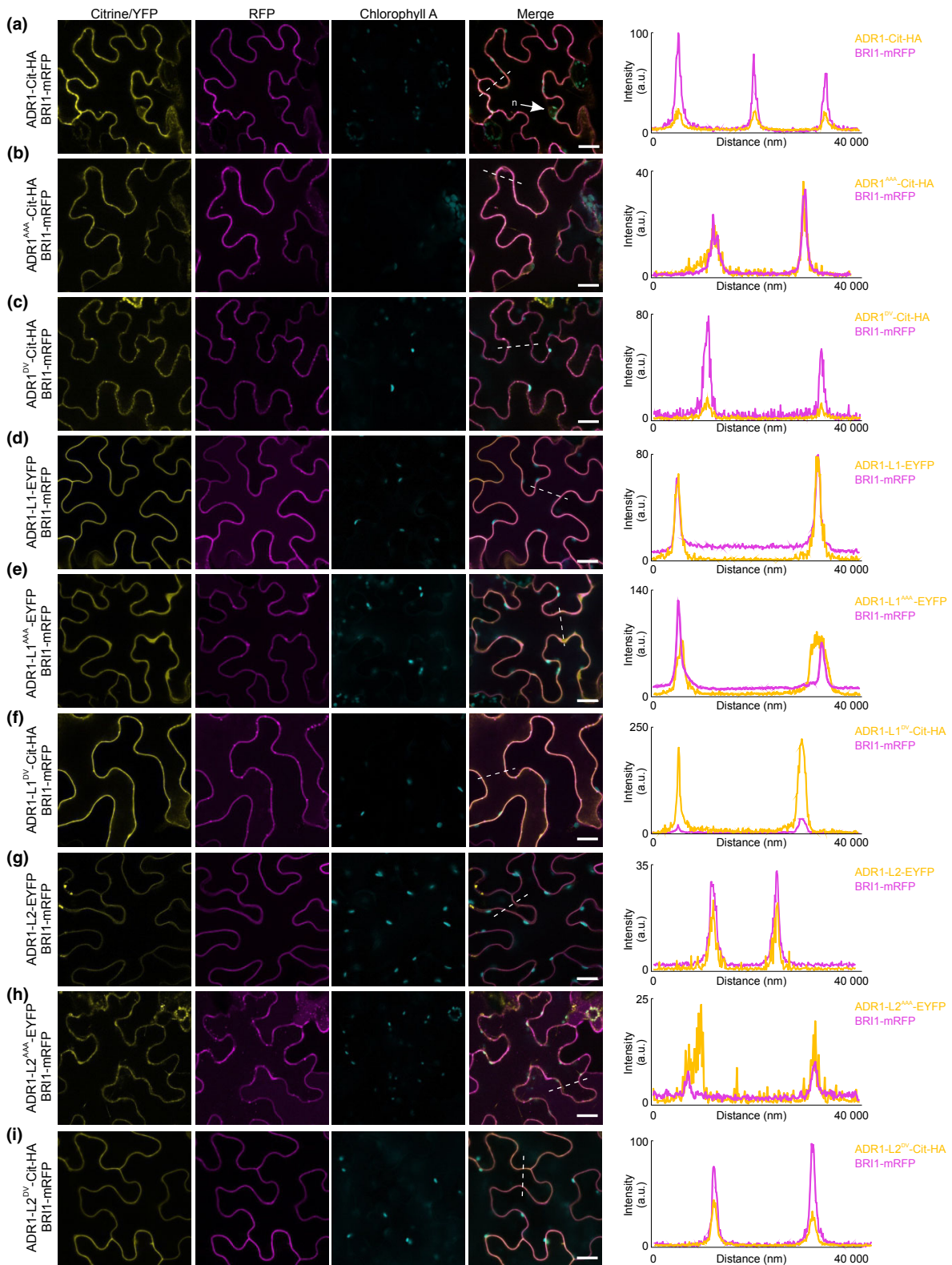
Fig. 1 AtADR1 proteins mainly localize to the plasma membrane (PM). Single plane secant views showing that AtADR1 proteins (ADR1, ADR1-L1, ADR1-L2) and auto-activated QHD (DV) mutants localize mainly to the PM, whereas the AtADR1 P-loop (AAA) mutants additionally display cytosolic and endoplasmic reticulum (ER) localization. The indicated ADR1 proteins fused to Citrine-HA or EYFP were transiently co-expressed with the PM-resident protein BRI1-mRFP in *Nicotiana benthamiana* leaves and confocal imaging was done at 4 h (a, b, c, f) or 5 h (i) post-estradiol induction or 2 d post-infiltration (d, e, g, h). Localization of ADR1s is shown with the first column (Citrine/YFP, in yellow) and the co-localized PM-localized BRI1 is shown in the second column (RFP, in magenta). Chloroplasts are shown in the third column (chlorophyll *A*, in cyan) and the merged images are shown in the fourth column (merge). Fluorescence intensities were measured along the dotted line depicted in the merge images. Bars, 20 μm; n, nucleus.
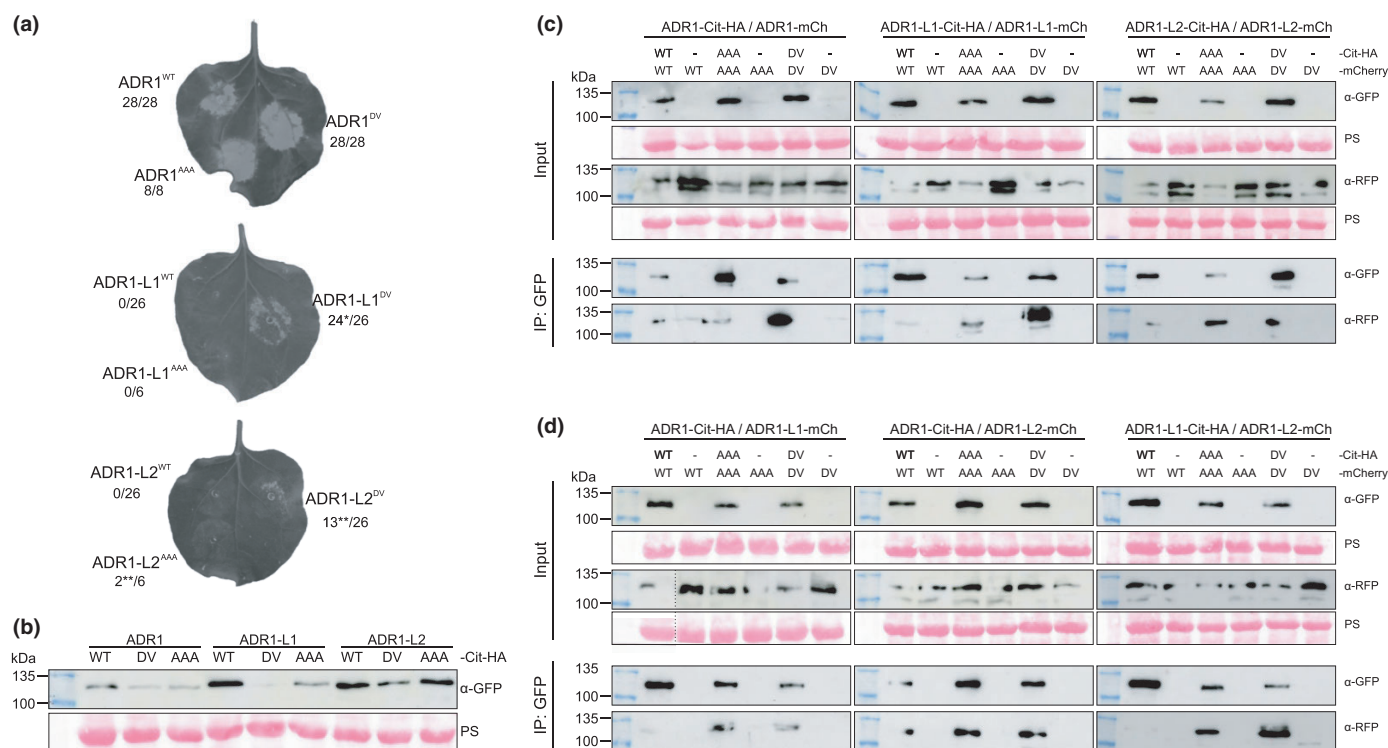
Fig. 2 Homo- hetero-association of AtADR1 proteins. Characterization of the wild-type (WT), P-loop (AAA) and QHD (DV) variants of AtADR1 proteins. (a) Transient expression of steady-state (WT), P-loop mutant (AAA) or auto-activated mutant (DV) AtADR1s-Citrine-HA fusion proteins in *Nicotiana benthamiana*. Photographs were taken under ultraviolet (UV) light at 23 h post-estradiol induction and 47 h post-infiltration. White/light grey areas correspond to dead leaf tissue. Numbers represent the number of leaves showing cell death out of the number of leaves analysed. Asterisk indicates weak cell death. Double-asterisk indicates very weak cell death. Images of the same leaves under normal light are shown in Supporting Information Fig. S3. (b) Immunoblot analysis of the transiently expressed proteins (see (a)) using anti-GFP antibody. Equal loading of the proteins is indicated by the Rubisco band from the Ponceau staining (PS). Proteins were extracted 3 h post-estradiol induction. (c, d) AtADR1 proteins form both homo-dimers (c) and hetero-dimers (d). The indicated proteins were transiently co-expressed in *N. benthamiana* and leaf tissue was harvested 3 h post-estradiol induction. Total proteins were immunoprecipitated with anti-GFP beads and immunoblotted with anti-GFP and anti-RFP antibody, respectively. Immunoblots using total proteins before immunoprecipitation are shown as input (upper panel) and immunoprecipitated proteins are shown as IP (lower panel). Equal loading of the proteins is indicated by the Rubisco band from the PS. Co-immunoprecipitation was repeated two times with similar results. For ADR1^{WT}/ADR1-L1^{WT} interaction, ADR1^{WT}-Cit-HA from the flow-through is shown as input since we were not able to detect it in the input fraction. ADR1^{DV}, ADR1^{D461V}; ADR1-L1^{DV}, ADR1-L1^{D489V}; ADR1-L2^{DV}, ADR1-L2^{D484V}; ADR1^{AAA}, ADR1^{212AAA214}; ADR1-L1^{AAA}, ADR1-L1^{212AAA214}; ADR1-L2^{AAA}, ADR1-L2^{212AAA214}; IP, immunoprecipitation.

very weak cell death response that was not reliably reproducible (only 13 of 26 leaves showed mild or weak HR-like symptoms; Figs 2a,b, S3). We also found that the AtADR1-induced HR-like cell death occurred earlier in comparison to the cell death response triggered by both AtADR1-L1^{DV} and AtADR1-L2^{DV}. AtADR1-L1 and AtADR1-L2 WT proteins did not induce a cell death response. The same applies to the catalytic P-loop mutant (AAA) AtADR1-L1^{AAA}, whereas AtADR1-L2^{AAA} did sometimes, but not strongly and reliably induce a cell death response under our conditions (Figs 2a,b, S3). By contrast, AtADR1^{AAA} consistently induced a strong cell death response in all our experiments, suggesting that P-loop function is not required for at least AtADR1 cell death activity. These observations suggest that some RNLs may not require a functional P-loop for their immune activity.

Our data indicate that WT AtADR1 is already highly active under steady-state conditions, whereas AtADR1-L1 and AtADR1-L2 are kept inactive. However, exchange of D for V in the QHD motif renders AtADR1-L1^{DV} and AtADR1-L2^{DV} into active proteins.

We next analysed whether AtADR1s WT and mutant variants are capable of forming homo- and hetero-oligomers by co-immunoprecipitation experiments. Therefore, differently tagged AtADR1s WT and mutant proteins were transiently co-expressed in *N. benthamiana*. Our co-immunoprecipitation experiments revealed that all AtADR1 WT and mutant proteins self-associated (Fig. 2c). While AtADR1 WT proteins strongly self-associated, the capability of AtADR1-L1 and AtADR1-L2 WT proteins to homo-dimerize seems to be reduced. Exchange of D for V in AtADR1 and AtADR1-L1 clearly increased the amount of the co-immunoprecipitated AtADR1 and AtADR1-L1, respectively (Fig. 2c). Interestingly, the P-loop mutations (AAA) did not abolish self-association capability. We even observed enhanced self-association, in particular of AtADR1-L1^{AAA} and AtADR1-L2^{AAA} compared to their WT proteins (Fig. 2c). Likewise, we found that AtADR1 proteins are also capable of forming hetero-dimers and that the hetero-association is positively affected by mutations in both the P-loop regions and QHD motifs of all three AtADR1s, respectively (Fig. 2d).

Taken together, AtADR1 proteins associate into homomeric and heteromeric complexes, suggesting that they might exist as dimers/oligomers when inducing cell death. However, homo- and hetero-associations seemed to be stabilized by mutations in both the P-loop region and the QHD motif. Mutations in both regions might interfere with intramolecular interactions, resulting in a conformational change that might favour, promote or stabilize RNL–RNL interactions.

AtADR1s and CNL RPM1 localization and protein stability require PM PI4P

The PM localization of AtADR1, AtADR1-L1 and AtADR1-L2 suggests that they execute their immune function at this cellular compartment as observed for other NLRs, such as AtRPM1 or AtZAR1 and the RNL AtNRG1.1 (Gao *et al.*, 2011; Bi *et al.*, 2021; Jacob *et al.*, 2021). Interestingly, for both RNL families and many PM-localized CNLs, including AtRPM1, no transmembrane region could be identified and thus, they are most likely peripheral membrane proteins (Table S2) (Boyes *et al.*, 1998). Given the structural homology of RNL CC_R domains with the phosphatidyl-inositol phosphate binding HeLo domain of mammalian MLKL (Dondelinger *et al.*, 2014; Jacob *et al.*, 2021), we investigated whether the presence of specific phosphoinositide species might be important for the PM localization of AtADR1s and the CNL AtRPM1. Since PI4P is one of the major phospholipids of the plant PM (Simon *et al.*, 2016), we tested whether AtADR1s and AtRPM1 PM localization require PI4P. Transient expression of the catalytic domain of the PM-localized PI4P-specific yeast phosphatase SAC1p can be used to specifically decrease the PI4P pool at the PM and therefore, to determine the requirement of PI4P for the PM localization and function of proteins of interest (Simon *et al.*, 2016; Gronnier *et al.*, 2017; Doumane & Caillaud, 2020). We co-expressed the three AtADR1s and AtRPM1 with SAC1 and determined their subcellular localization and protein abundance by confocal microscopy and Western blot analysis, respectively. The N-terminally myristoylated and PM localized Arabidopsis CNL AtRPS5 was included as a control NLR as AtRPS5 PM localization (and function) was not expected to be affected by PM PI4P reduction (Qi *et al.*, 2012; Pottinger & Innes, 2020). Co-expression with the WT SAC1 (SAC1^{WT}), but not with the catalytically inactive SAC1 (SAC1^{dead}), affected the PM localization of all tested NLRs except AtRPS5 (Figs 3a,c,e,g, S4a). Thus, the effect of SAC1 activity on the PM localization of AtADR1s and AtRPM1 is specific and not of general nature. Co-localization of AtADR1 with SAC1^{WT} at the PM was rarely detectable and the majority of AtADR1 was localized inside the cell, likely at the ER and/or cytosol (Fig. 3a). However, no fluorescence was observed for either AtADR1-L1 or AtRPM1, and only a very weak fluorescence was detectable in the cell for AtADR1-L2, after co-expression with SAC1^{WT} (Fig. 3c,e,g). Western blot analysis of AtADR1-L1, AtADR1-L2 and AtRPM1 confirmed a remarkable or even a complete loss of NLR protein accumulation upon co-expression with SAC1^{WT} (Fig. 3d,f,h). By contrast, AtADR1 displayed a slightly reduced accumulation in Western blot analysis when co-expressed with SAC1^{WT} (Fig. 3b). These findings indicate that depleting the PM PI4P pool severely affects the localization and consequently, protein accumulation of AtADR1-L1, AtADR1-L2 and AtRPM1. A similar observation was previously reported for a PS specific binding protein, which is unstable in the Arabidopsis *pss1* mutant that is impaired in PS production (Platre *et al.*, 2018). By contrast, though depletion of PI4P from the PM severely affected the subcellular localization of AtADR1, AtADR1 protein abundance was only marginally reduced. 82% of AtADR1 was still detectable by protein blot analysis upon co-expression with SAC1^{WT}.

In order to test whether the reduced or complete loss of NLR protein accumulation upon SAC1^{WT} co-expression was due to degradation of the mis-localized proteins, we analysed protein levels by Western blot in presence of both protease and proteasome inhibitors. The specific inhibition of proteasomal degradation by BTZ had an observable effect on the accumulation of AtADR1 and AtADR1-L2 (Fig. S5a,c) and a weak effect on AtADR1-L1 (Fig. S5b). This indicates that proteasomal degradation is, at least partially, responsible for the degradation of mis-localized AtADR1s. By contrast, mis-localized AtRPM1 could not be stabilized in the presence of BTZ (Fig. S5d), suggesting that the proteasome plays no major role in AtRPM1 degradation. This is consistent with previously published data (Gao *et al.*, 2011).

Together these results clearly demonstrate that all three AtADR1s and AtRPM1 require PI4P or a high electronegativity driven by PI4P at the PM for their proper localization and that loss of PM localization severely affects their protein stability. Degradation of the mis-localized NLRs is, at least for the AtADR1s, partially mediated by the proteasome.

Cell death function of PM-localized AtADR1s and CNL AtRPM1 is PI4P dependent

Plasma membrane localization of several NLRs, including AtRPM1, was shown to be important for their immune and cell death function (Gao *et al.*, 2011; Qi *et al.*, 2012; El Kasmi *et al.*, 2017; Wang *et al.*, 2019a, 2020a). The severe effect of PI4P depletion from the PM on the localization and stability of the AtADR1s and AtRPM1, prompted us to analyse whether their cell death function was also affected.

To examine this, we co-expressed SAC1^{WT} or SAC1^{dead} with the cell death-inducing AtADR1 WT and AtADR1^{DV} mutant (Fig. 4a,b). Co-expression with SAC1^{WT}, but not with SAC1^{dead}, suppressed the cell death response of both AtADR1 WT (Fig. 4a) and AtADR1^{DV} (Fig. 4b). We conclude that PI4P depletion severely affects AtADR1 cell death activity, most likely due to loss or severe reduction of PM localization, as ADR1 protein abundance was not massively affected (Figs 3a,b, 4a).

AtRPM1 guards the immune regulatory protein RIN4 (RPM1 INTERACTING PROTEIN 4) and is activated by an effector-triggered phosphorylation of RIN4 threonine 166 (Chung *et al.*, 2011; Liu *et al.*, 2011). AtRPM1 activation can be reconstituted in *N. benthamiana* by co-expression of AtRPM1 and a
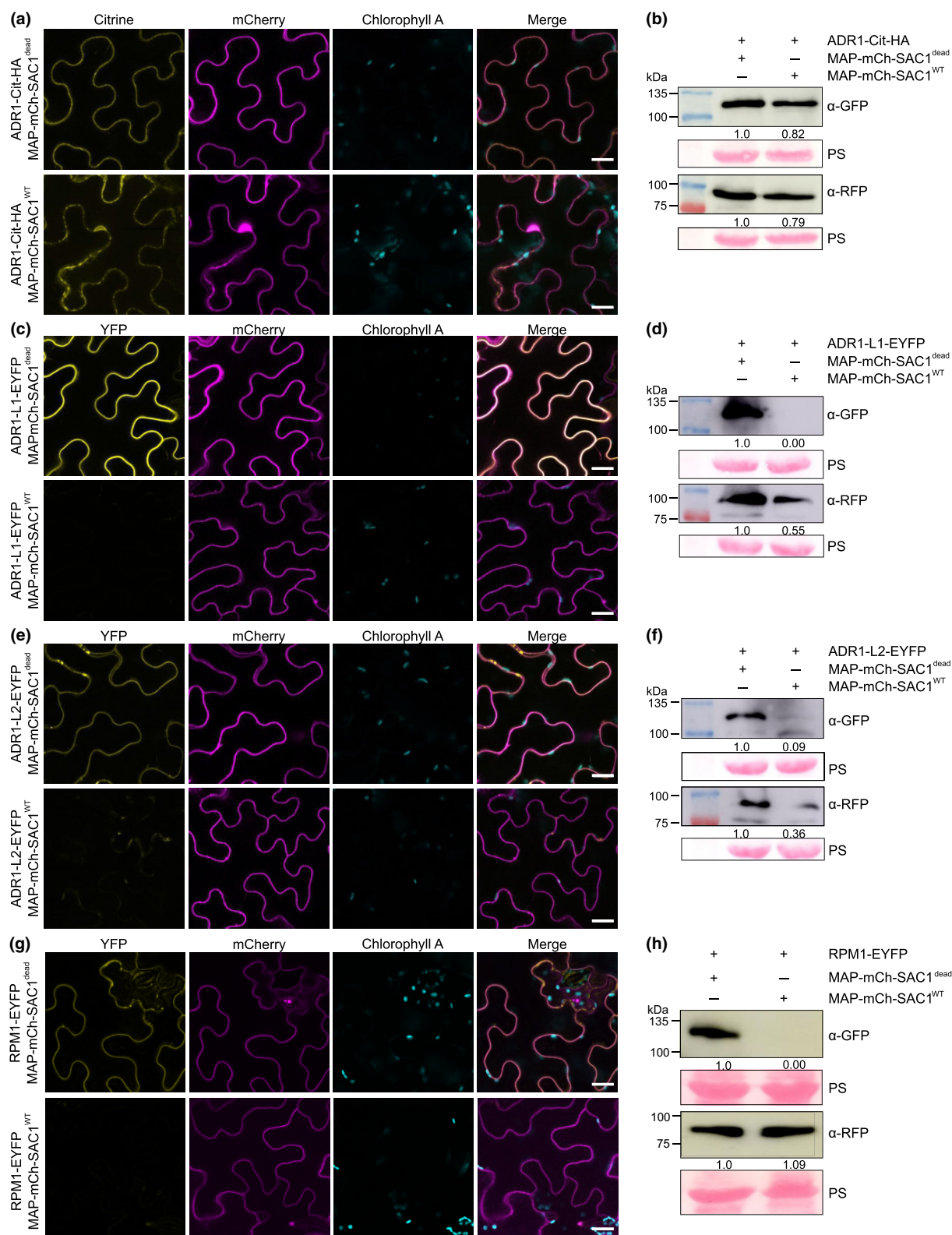
phosphomimic mutant of AtRIN4 (AtRIN4^{T166D}) (Gao *et al.*, 2011; Chung *et al.*, 2014). The strong cell death response upon AtRPM1 activation by AtRIN4^{T166D} was completely inhibited by SAC1^{WT} co-expression, but not by SAC1^{dead} (Fig. 4c). Cell death activity of effector-activated AtRPM1 was also severely affected by SAC1^{WT} co-expression (Fig. S6b), suggesting that AtRPM1-mediated cell death activity requires PM localization and consequently, depends on the PM PI4P pool.

Fig. 3 Phosphatidylinositol-4-phosphate (PI4P) depletion reduces plasma membrane (PM) localization and stability of AtADR1s and AtRPM1. Effects on the localization and stability of AtADR1s (ADR1, ADR1-L1, ADR1-L2) and AtRPM1 after transient co-expression with SAC1^{dead} (upper panel) or SAC1^{WT} (lower panel). (a) MAP-mCherry-SAC1^{WT} co-expression affects ADR1-Citrine-HA PM localization but not its endoplasmic reticulum localization. (c, e, g) ADR1-L1-, ADR1-L2- and RPM1-EYFP fluorescence is not (c, g) or only weakly (e) detectable when co-expressed with MAP-mCherry-SAC1^{WT}. Fusion proteins were transiently expressed in *Nicotiana benthamiana* leaves and confocal imaging was done at 4 h after estradiol induction (a), 2 d post-infiltration (c, e) or 24 h post-infiltration (g). Localization of ADR1-Citrine-HA and ADR1-L1-, ADR1-L2- and RPM1-EYFP proteins is shown in the first column (Citrine/YFP, in yellow) and MAP-mCherry-SAC1^{WT} or MAP-mCherry-SAC1^{dead} is shown in the second column (mCherry, in magenta). Chloroplasts are shown in the third column (chlorophyll A, in cyan) and the merged images are shown in the fourth column. Images are single plane secant views. Bar, 20 µm. (b) Immunoblot analysis indicates a slightly reduced accumulation of ADR1-Citrine-HA after co-expression with MAP-mCherry-SAC1^{WT} compared to co-expression with MAP-mCherry-SAC1^{dead}. (d, f, h) Co-expression of ADR1-L1 (d), ADR1-L2 (f) and RPM1 (h) -EYFP with MAP-mCherry-SAC1^{WT} severely affects their stability. Immunoblot analysis of the transiently expressed proteins (see (a), (c), (e), (g)) using anti-GFP and anti-RFP antibody, respectively, are shown. Equal loading of the proteins is indicated by the Rubisco band from the Ponceau staining (PS). Numbers show quantification of band intensities normalized to the Rubisco band from the PS. Protein samples were collected at 4 h after estradiol induction (b), 2 d post-infiltration (d, f) or 24 h post-infiltration (h).

To demonstrate that the effect of decreasing the PM PI4P pool on the cell death activity of AtADR1s and AtRPM1 is specific and not of general nature, we analysed whether SAC1^{WT} activity affects cell death mediated by the myristoylated and 'constitutively' PM localized AtRPS5. Similar to the AtRPM1-mediated cell death response, the AtRPS5-mediated and effector-triggered cell death can be reconstituted in transient expression assays in *N. benthamiana* (Ade *et al.*, 2007). Neither the expression of SAC1^{WT} nor SAC1^{dead} suppressed effector-triggered and AtRPS5-mediated cell death (Fig. S4e). These results suggest that the effect of SAC1 activity on cell death induction by the AtADR1s and AtRPM1 is specific.

Transient over-expression of the CC$_R$ domains of the AtRNLs AtADR1, AtADR1-L2 and AtNRG1.1 is sufficient to induce a cell death response in *N. benthamiana* (Fig. 4d–f) (Collier *et al.*, 2011). CC$_R$ domain induced cell death activity was dramatically diminished by SAC1^{WT}, but not SAC1^{dead} co-expression (Fig. 4d–f), similar as observed for full-length AtADR1. These results suggest that the RNL CC$_R$ domains also induce cell death at the PM and that their activity is affected by PM PI4P depletion. Expression of the AtADR1-L1 CC$_R$ domain did not induce a visible cell death response in transient expression assays under our conditions and hence, could not be tested for PI4P dependency (Fig. S6a). Interestingly, in contrast to the measurable negative effect of SAC1^{WT} activity on the accumulation of the full-length NLR proteins (Fig. 3d,f,h) we did not observe a similar effect on the CC$_R$ domains (Fig. 4d–f). Altogether, PI4P depletion does not affect CC$_R$ domain stability, but substantially affects CC$_R$ domain-induced cell death.

Taken together, our results demonstrate that AtRNL and AtRPM1 cell death activity is significantly affected by PI4P depletion from the PM and further suggest that cell death activity of all AtRNLs, including the partially ER-localized AtNRG1s (Lapin *et al.*, 2019; Wu *et al.*, 2019; Jacob *et al.*, 2021), takes place at the PM.

PI4P depletion affects PM localization of AtADR1, AtADR1-L1 and AtADR1-L2 CC$_R$ domains

Cell death activity of the AtADR1 and AtADR1-L2 CC$_R$ domains was notably diminished by SAC1^{WT} co-expression (Fig. 4d,e). However, unlike the full length AtADR1s, the stability of the AtADR1s CC$_R$-domains was not affected (Fig. 4d,e). To test

whether PI4P depletion affects AtADR1s CC$_R$ localization and hence function, we co-expressed the CC$_R$ domains of all three AtADR1s with SAC1^{WT} or SAC1^{dead} and analysed their localization by confocal microscopy. The AtADR1s CC$_R$ domains showed a similar localization pattern as their 'parental' full-length proteins. All three CC$_R$ domains localized to the PM in the presence of SAC1^{dead} (Figs 5, S7). We also observed that the AtADR1 CC$_R$ domain localized to dot-like structures and to ER membranes (Figs 5a, S7a). However, the PM localization of all three AtADR1s CC$_R$ domains was affected by SAC1^{WT} co-expression. Fluorescence of the CC$_R$ domains was detected at intracellular puncta and also at ER membranes and/or the cytosol (Figs 5, S7).

Taken together, PI4P depletion from the PM leads to a reduced PM localization (and loss of cell death function) of the AtADR1s CC$_R$ domains and potentially a (mis-)localization to endosomal compartments and the ER or cytosol. Proteins that are normally interacting with the PM in a PI4P- or electronegativity-dependent manner have been shown to 'adopt' endosomal localization once the PM PI4P pool is depleted (Simon *et al.*, 2016; Platre *et al.*, 2018).

AtADR1, AtADR1-L1, AtADR1-L2 CC$_R$ and AtRPM1 CC domains specifically interact with anionic lipids *in vitro*

Reducing the abundance of PM PI4P levels negatively influenced the function, localization and stability of the tested AtADR1s and AtRPM1. Thus, it is very likely that a direct interaction of AtADR1s and AtRPM1 with PM PI4P or other anionic lipids is causal for their PM localization. Given the structural homology of the CC$_R$ domains with the N-terminal HeLo domain of MLKL (Jacob *et al.*, 2021) and the importance of the CC domain for cell death function of many CNLs (Bentham *et al.*, 2018) we investigated whether the AtADR1s CC$_R$ and the AtRPM1 CC domains bind to specific phospholipids. We generated C-terminally HA-tagged CC domain proteins *in vitro* and incubated the proteins on a lipid array (PIP strip). As a negative control we included *in vitro* transcribed and translated Citrine-HA. All three AtADR1s CC$_R$ domains and the AtRPM1 CC domain directly interacted with phospholipids carrying polyacidic headgroups and hence, bound to all PIPs and PA (Fig. 6a–d). For the AtADR1s CC$_R$ domains we additionally observed a weak interaction with the anionic and low abundant
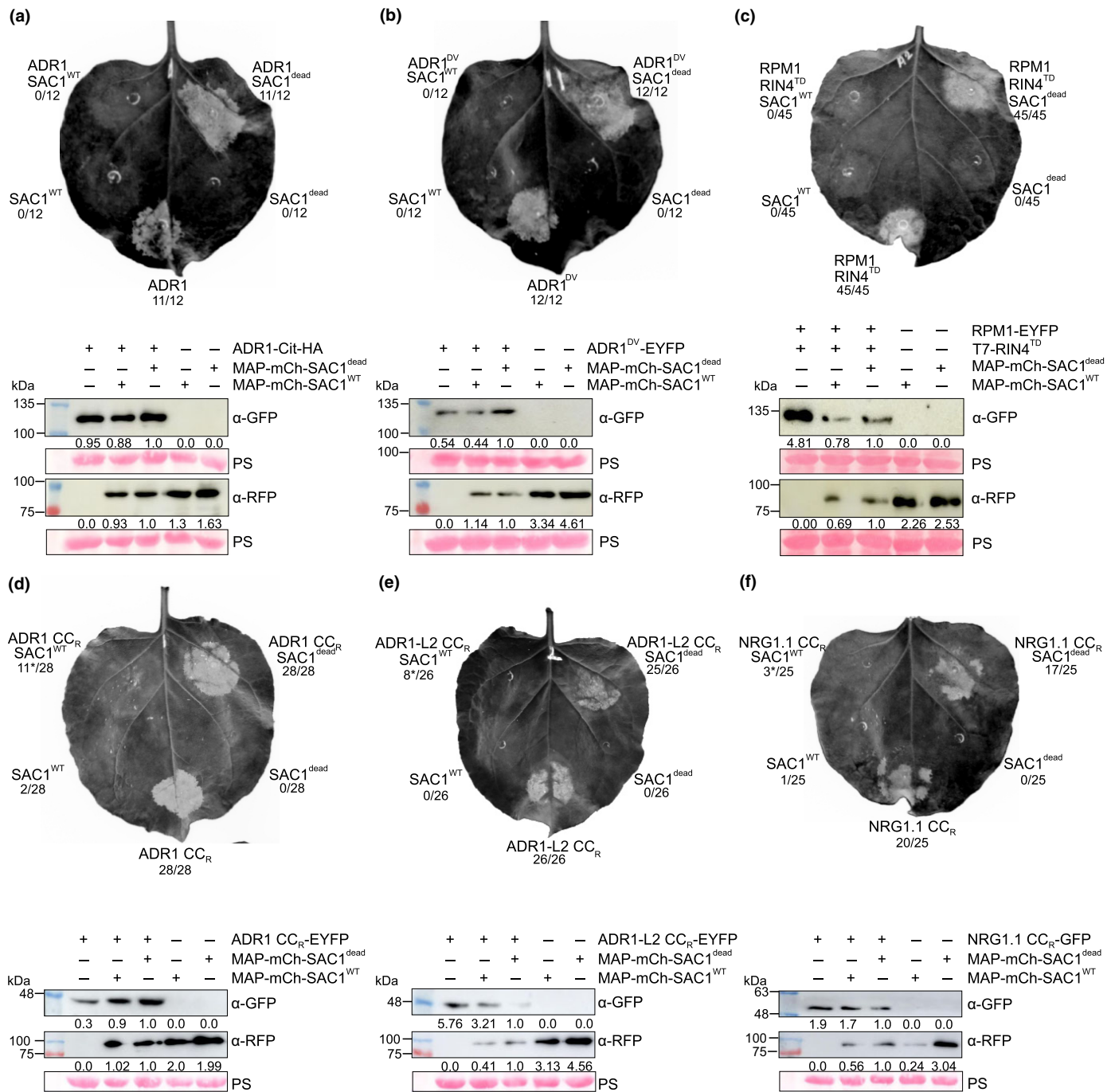
Fig. 4 MAP-mCherry-SAC1 strongly affects AtADR1s and AtRPM1 cell death activity. Cell death activity of full-length AtADR1 and the autoactive AtADR1^{DV} mutant, the phospho-mimic T7-RIN4^{T166D} activated RPM1 as well as the autoactive AtADR1s CC$_R$ domains (ADR1 CC$_R$ and ADR1-L2 CC$_R$), is suppressed by SAC1^{WT} co-expression. (a–f, upper panels) Transient expression of ADR1 (a), ADR1^{D461V} (b), phospho-mimic T7-RIN4^{T166D} (RIN4^{TD})-activated RPM1 (c), ADR1 CC$_R$ (d), ADR1-L2 CC$_R$ (e) and NRG1.1 CC$_R$ (f) Citrine-HA- or EYFP-fusion proteins in *Nicotiana benthamiana* co-expressed with MAP-mCherry-SAC1^{WT} or MAP-mCherry-SAC1^{dead}. Images of leaves were taken under ultraviolet (UV) light at 8 h post-estradiol induction (a), 30 h post-infiltration (hpi) (b), 24 hpi (c), 23 hpi (d), 26 hpi (e) and 28 hpi (f). Phospho-mimic T7-RIN4^{T116D} was co-expressed to activate RPM1. White/light grey areas on the leaves indicate dead tissue. Numbers represent the number of leaves showing cell death out of the number of leaves analysed. Asterisk indicates weak cell death. (a–f, lower panels), Immunoblot analysis of the transiently expressed proteins (see upper panels) using anti-GFP and anti-RFP antibody, respectively. Membranes were horizontally cut into two pieces and probed with anti-GFP or anti-RFP antibody, respectively (a–c). Equal loading of the proteins is indicated by the Rubisco band from the Ponceau staining (PS). Numbers show quantification of band intensities normalized to the Rubisco band from the Ponceau staining. Protein samples were collected at 24 hpi (a), 4 h post-estradiol induction (b), 22 hpi (c) or 20 hpi (d–f).
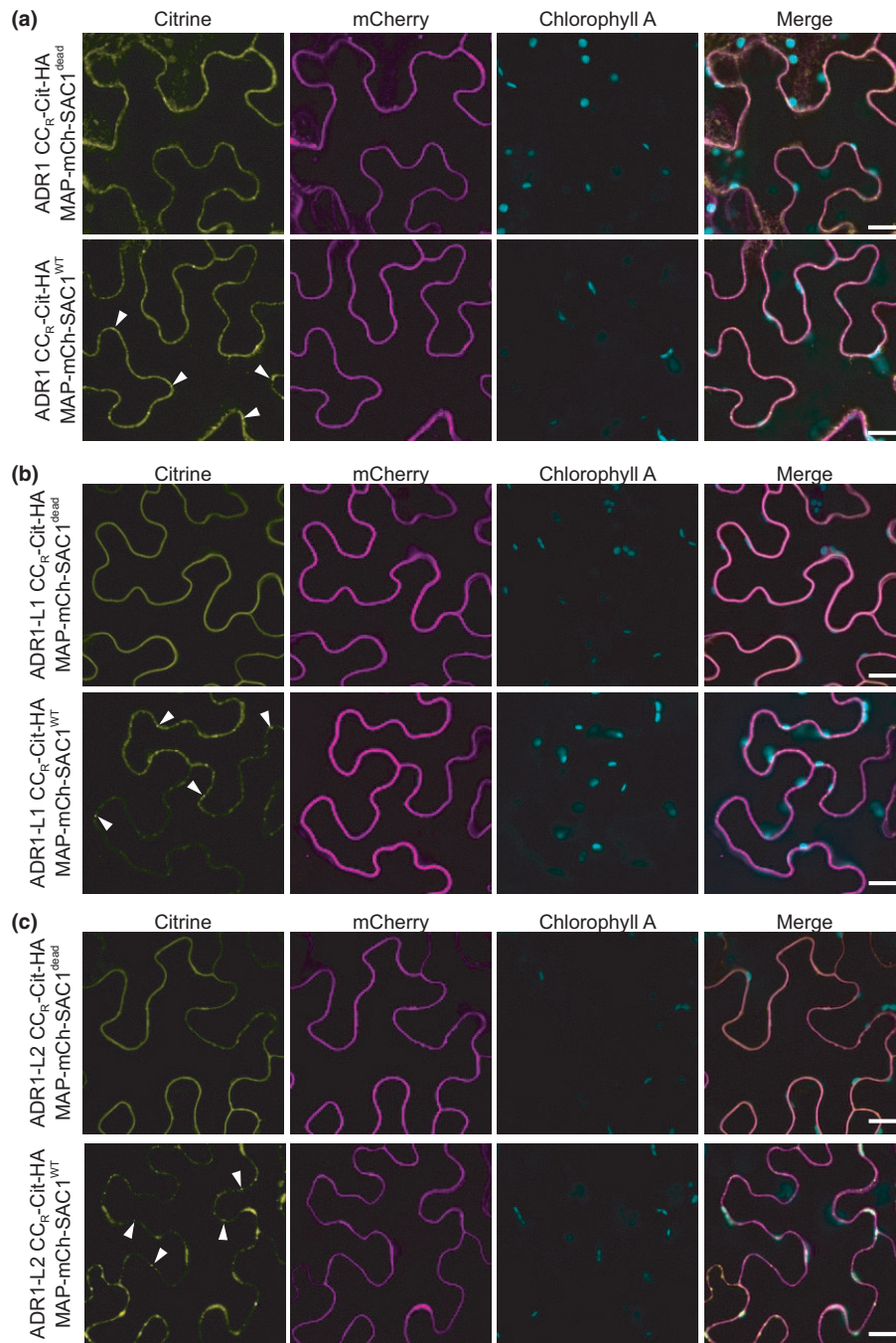
Fig. 5 Phosphatidylinositol-4-phosphate (PI4P) depletion affects plasma membrane (PM) localization of AtADR1 CC_R domains. Co-expression of SAC1^{WT} noticeably affects ADR1 CC_R (a), ADR1-L1 CC_R (b) and ADR1-L2 CC_R (c) localization. (a–c) Citrine-HA tagged AtADR1 (ADR1, ADR1-L1, ADR1-L2) CC_R domains were transiently co-expressed with MAP-mCherry-SAC1^{dead} (upper panels) or MAP-mCherry-SAC1^{WT} (lower panels) in *Nicotiana benthamiana* leaves and confocal imaging was done at 3 h (a) or 4 h (b, c) post-estradiol induction. MAP-mCherry-SAC1^{WT} induces ADR1 CC_R, ADR1-L1 CC_R and ADR1-L2 CC_R re-localization to intracellular puncta, most likely endosomes (white arrowheads in lower panels of a–c). Localization of ADR1 CC_R-Cit-HA domains is shown with the first column (Citrine, in yellow) and MAP-mCherry-SAC1^{dead} or MAP-mCherry-SAC1^{WT} is shown in the second column (mCherry, in magenta). Chloroplasts are shown in the third column (chlorophyll *A*, in cyan) and the merged images are shown in the fourth column (merge). Images are single plane secant views. Bar, 20 μm.

PS (Fig. 6a–c) (Colin & Jaillais, 2020). We also detected a very weak interaction of Citrine-HA to PIPs, but much weaker than observed for the AtADR1s CC_R and AtRPM1 CC domains (Fig. 6e). These results suggest a strong binding of the AtADR1s and AtRPM1 CC_R/CC domains to negatively charged polyacidic phospholipids most likely via an electrostatic interaction.

PI(4,5)P$_2$ depletion has no impact on PM localization and cell death function of AtADR1s and AtRPM1

The strong effect of PI4P depletion at the PM on the function and localization of AtADR1s and AtRPM1 and the specific interaction of their CC_R/CC domains with anionic lipids (including
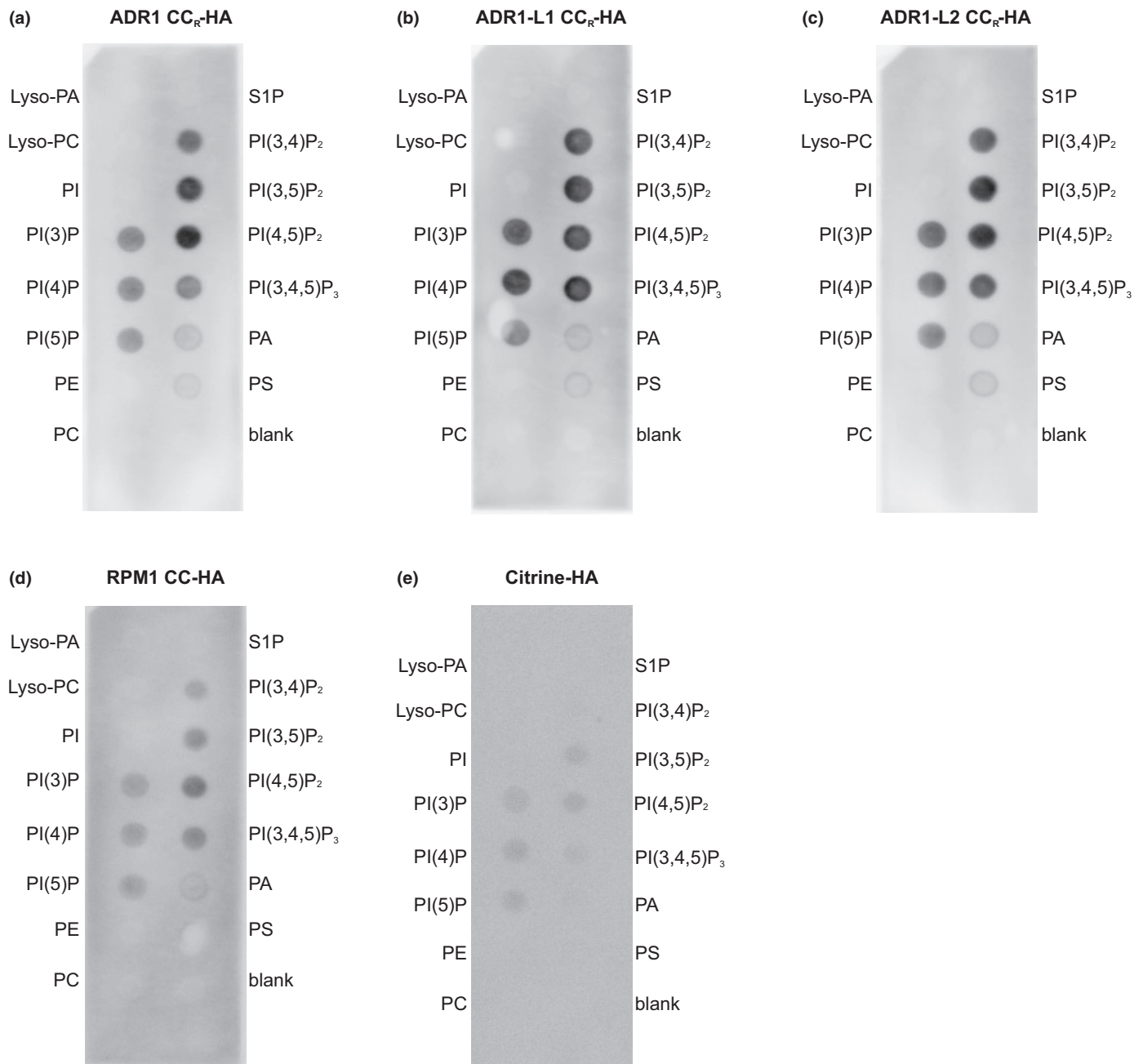
Fig. 6 AtADR1s CC_R and AtRPM1 CC interact *in vitro* with anionic lipids. Arabidopsis ADR1s CC_R and RPM1 CC domains can directly bind to anionic lipids *in vitro*. *In vitro* transcribed and translated AtADR1 CC_R (a), AtADR1-L1 CC_R (b), AtADR1-L2 CC_R (c), AtRPM1 CC (d) domains and Citrine (e) fused with a C-terminal single haemagglutinin (HA) tag were incubated with a commercial phosphatidylinositol phosphate (PIP) strip. Binding was analysed by immunoblotting with anti-HA antibody. The analysed CC_R domains bind strongly and the RPM1 CC domain binds weakly to PI(3)P, PI(4)P, PI(5)P, PI(3,4)P2, PI(3,5)P2, PI(4,5)P2 and PI(3,4,5)P3. A weak interaction of the AtADR1s CC_R domains was also detected with phosphatidic acid (PA) and phosphatidylserine (PS). Citrine (negative control) showed a very weak association with PI(3)P, PI(4)P, PI(5)P, PI(3,5)P2, PI(4,5)P2 and PI(3,4,5)P3.

PI4P) *in vitro*, suggest that PI4P plays a major role for their interaction with and consequently, for their function at the PM. PI(4,5)P_2 fulfils similar important cellular functions, is specifically found at the plant PM, and is also required for the PM association of many proteins (Doumane *et al.*, 2020), like the mammalian MLKL protein (Dondelinger *et al.*, 2014; Quarato *et al.*, 2016). However, PI(4,5)P_2 is not required for plant PM electronegativity (Simon *et al.*, 2016). Our observation of the additional direct binding of the AtADR1s CC_R and AtRPM1 CC domains to PI(4,5)P_2 (Fig. 6), prompted us to test whether PI(4,5)P_2 is also required for AtADR1s and AtRPM1 PM localization and cell death function. We co-expressed the PM-anchored WT PI(4,5)P_2 5-phosphatase domain from the Drosophila OCRL protein (dOCRL^{WT}) that specifically depletes the PI(4,5)P_2 pool at the plant PM (Doumane *et al.*, 2020) with AtADR1, AtADR1-L1, AtADR1-L2, AtRPM1 and AtRPS5. As

a control we co-expressed a phosphatase dead mutant version of dOCRL (dOCRL^{dead}) that is catalytically inactive (Doumane *et al.*, 2020). Co-expression of dOCRL^{WT} or dOCRL^{dead} with AtADR1s, AtRPM1 and AtRPS5 had no visible effect on their (PM-) localization or protein accumulation (Figs S4c,d, S8). Co-expression of dOCRL^{WT}, but not of the catalytically inactive dOCRL^{dead}, with the cell death-inducing CC$_R$ domains of AtADR1, AtADR1-L2 and AtNRG1.1 did not inhibit their activity and a cell death induction was visible for all three CC$_R$ domains (Fig. S9a–c). Similarly, depleting the PI(4,5)P$_2$ pool from the PM did not affect AtADR1 and AtADR1^{DV}-induced cell death responses (Fig. S9d,e). Further, we found no inhibition of the cell death activity of AtRPM1 or AtRPS5 in either the presence of dOCRL^{WT} or dOCRL^{dead} (Figs S4f, S6c, S9f). Consistent with the fact that PI(4,5)P$_2$ depletion does not affect AtRNL and AtRPM1-mediated cell death, we also did not observe a negative effect on protein accumulation by PM PI(4,5)P$_2$ depletion (Figs S8, S9). This suggests that AtRNLs, AtRPM1 and AtRPS5 PM localization and their PM-coupled cell death function is independent of PI(4,5)P$_2$.

Collectively, this demonstrates that PI(4,5)P$_2$ is likely not a major contributor for AtADR1s, AtRPM1 and AtRPS5 localization and function at the PM.

Discussion

Upon effector-induced activation, the CNL AtZAR1 oligomerizes and translocates to the PM where it forms a pore-like structure via the alpha 1 helix of its CC domain that acts as a cation selective channel to induce a cell death and immune response (Wang *et al.*, 2019a,b; Bi *et al.*, 2021). PM or endomembrane localization was shown to be necessary for the cell death and immune function of many CNLs (Gao *et al.*, 2011; Engelhardt *et al.*, 2012). Some CNLs localize to membranes via N-terminal myristoylation and/or palmitoylation, and the residues required for this post-translational modification were demonstrated to be important for the function of these CNLs (Qi *et al.*, 2012; Kawano *et al.*, 2014). However, the molecular mechanism underlying the localization of nonacylated PM/membrane-localized NLRs remains elusive. We present data that suggests a model in which AtADR1s and the CNL AtRPM1 require PI4P at the PM for proper localization that is required for protein stability and cell death function upon (auto-)activation (Fig. 7). The localization is most likely regulated by direct binding of their CC/CC$_R$ domains to anionic lipids (including the very abundant PI4P), possibly via positive charges in a basic hydrophobic stretch that we found in all the CC/CC$_R$ domains (Fig. S10). We, however, cannot rule out the possibility that other mechanisms and/or domains are also required, for example the interaction with other (structural) lipids or integral membrane proteins. In this context, it has recently been shown that AtADR1s interact with a member of the receptor-like kinase family (Pruitt *et al.*, 2021). However, the strong effect of PI4P depletion from the PM on NLR localization and function, suggests that PI4P contributes significantly to AtADR1s and AtRPM1 PM localization. By contrast, PI4P does not or only marginally contribute to the PM localization of
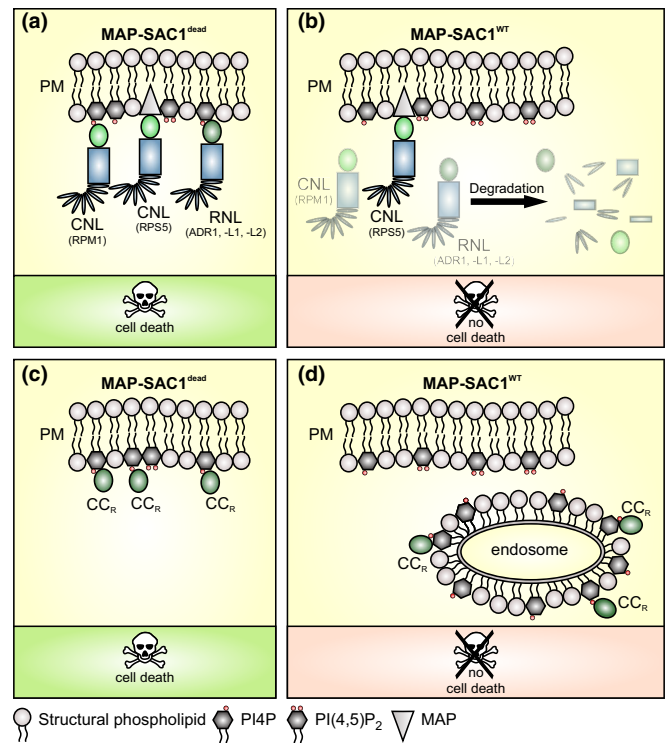

Fig. 7 Proposed model of AtADR1s and the CNL RPM1 localization and cell death/resistance function at the plasma membrane (PM). Localization of the RNLs AtADR1, AtADR1-L1 and AtADR1-L2 and nonacylated CNLs, here shown for AtRPM1, to the PM is mediated by a direct interaction of their CC$_R$ or CC domains with anionic lipids, of which phosphatidylinositol-4-phosphate (PI4P) is the most abundant at the plant PM. (a) Expression of catalytically inactive and forced PM-localized MAP-SAC1^{dead} does not affect AtADR1s, myristoylated (AtRPS5) or nonacylated CNL (AtRPM1) PM localization, and consequently also not their cell death activity upon (auto-)activation. (b) MAP-SAC1^{WT}-mediated PI4P depletion from the PM severely affects AtADR1s and nonacylated CNL AtRPM1, but not myristoylated CNL AtRPS5, localization. The decreased PI4P levels strongly affect PM electronegativity and this leads to a loss of binding to the PM and rapid degradation of AtADR1s and the nonacylated CNL AtRPM1. The reduced accumulation of AtADR1s and AtRPM1 in the cell consequently leads to loss of AtADR1s- and AtRPM1-mediated cell death induction. (c) The localization of AtADR1s CC$_R$ domains (ADR1 CC$_R$, ADR1-L1 CC$_R$, ADR1-L2 CC$_R$) is not affected by MAP-SAC1^{dead} expression, similar to full-length AtADR1s. Thus, there is no observable effect on CC$_R$ domain autoactivity (cell death induction). (d) PI4P depletion by MAP-SAC1^{WT} expression causes a re-localization of the AtADR1s CC$_R$ domains to intracellular puncta, probably endosomal compartments as their membranes might exhibit the highest electronegativity when MAP-SAC1^{WT} is expressed. This mis- or re-localization of AtADR1s CC$_R$ domains does not lead to their degradation. However, AtADR1s CC$_R$ cell death activity is severely reduced.

CNLs with myristoylation or acylation motifs, such as AtRPS5 (Fig. S4), and hence PI4P depletion does not affect their function.

Interestingly, recent studies demonstrated that there is a reduction in the PI4P levels and a specific enrichment of PI(4,5)P$_2$ on interfacial membranes during successful infections, like the extrahaustorial membrane (EHM) in Arabidopsis powdery mildew infections, the extra-invasive hyphal membrane (EIHM) in Arabidopsis *Colletotrichum* infections or at the potato (*Solanum tuberosum*) *Phytophthora infestans* infection sites (Shimada *et al.*,

New
Phytologist

2019; Qin *et al.*, 2020; Rausche *et al.*, 2020). The PI(4,5)P$_2$ enrichment at the EHM and EIHM is an essential susceptibility factor, which is most likely pathogen-induced and requires the function of the host phosphatidylinositol 4-phosphate 5-kinases (PIP5K) (Shimada *et al.*, 2019; Qin *et al.*, 2020). It is possible that the depletion of PI4P and the simultaneous enrichment of PI(4,5)P$_2$ at these host–pathogen interfaces result in a reduced accumulation of immune-regulatory proteins, for example NLRs, by removing possible binding sites and/or enhancing endocytosis of immune signalling components (Qin *et al.*, 2020). Plants however have evolved means to counteract this potentially pathogen/effector-induced enrichment of PI(4,5)P$_2$ by downregulating the activity of PIP5Ks or upregulating the activity of phosphoinositide 5-phosphatases upon pathogen perception by cell-surface localized immune receptors (Menzel *et al.*, 2019; Rausche *et al.*, 2020). Recently, it was also shown that members of the AtRPW8 protein family specifically localize to the EHM (Berkey *et al.*, 2017), and that the solanaceous helper NLR NRC4 (NLR REQUIRED FOR CELL DEATH 4) dynamically associates with the EHM during *P. infestans* infection (Duggan *et al.*, 2021), indicating that at least the RPW8/HR proteins and NRC4 may not require PI4P for membrane localization. Thus, actively changing or adjusting the lipid and protein composition and homeostasis of the plant PM is part of the evolutionary arms race between the host and the pathogen. This indicates the importance of the regulation/manipulation of lipid homeostasis and the associated changes in protein localization/stability in this battle.

Likewise, a correlation between the lipid composition of the PM and immunity as well as NLR (CNL) function and stability and an important function for phospholipase-dependent signalling in immunity was previously reported (Andersson *et al.*, 2006; Bargmann & Munnik, 2006; Johansson *et al.*, 2014; Yuan *et al.*, 2018; Schloffel *et al.*, 2020). Plant phospholipase families C (PLCs) and D (PLDs) are involved in many aspects of abiotic and biotic stress responses (Hong *et al.*, 2016). However, the exact mechanisms of how these enzymes and their product(s) influence immunity are not well understood (Li & Wang, 2019). Perception of pathogen-derived danger signals by NLRs and cell-surface localized pathogen-recognition receptors (PRRs) lead to the rapid activation and recruitment of PLDs and PLCs to pathogen entry sites at the PM as well as a biphasic transient calcium ion (Ca^{2+}) influx (Johansson *et al.*, 2014; Xing *et al.*, 2019; Schloffel *et al.*, 2020; Bi *et al.*, 2021; Jacob *et al.*, 2021). PLDs and PLCs induce the production of inositol polyphosphates, PA and diacylglycerol (DAG), all of which can function as second messengers during immunity as well as other stress responses (Li & Wang, 2019). The PLC- and PLD-mediated generation of PA is required for NLR-triggered reactive oxygen species (ROS) production and HR-like cell death, and external application of PA is sufficient to induce a cell death response and the transcriptional activation of the pathogen-responsive *PR1* promoter (Andersson *et al.*, 2006). The cation (Ca^{2+})-channel forming capability of some CNLs and RNLs at membranes is required for their cell death activity and downstream immune signalling (Jubic *et al.*, 2019; Wang *et al.*, 2020b; Bi *et al.*, 2021; Jacob *et al.*, 2021). In light of our results it is tempting to hypothesize that (1)

AtADR1s interact with PM/membrane anionic lipids, like PI4P, and that activation might lead to oligomerization (or at least stabilization of a higher order complex), and the formation of a cation-permeable channel/pore that (2) results in a transient Ca^{2+} influx and subsequently, in the (3) activation of Ca^{2+}-dependent and probably NLR-interacting phospholipases that (4) in turn produce lipid messengers, such as PA and DAG, which (5) might participate in the activation of downstream signalling components required for (6) NLR-mediated immune responses (Fig. S11) (Andersson *et al.*, 2006; Yuan *et al.*, 2018; Jubic *et al.*, 2019; Wang *et al.*, 2019a; Bi *et al.*, 2021; Jacob *et al.*, 2021).

Author contributions

SCS created RNL entry and destination constructs, performed confocal and cell death analysis for all RNLs, the co-immunoprecipitation experiments, the *in vitro* transcription and translation assay, the PIP strip analysis and all Western blot analysis for the RNL experiments and the degradation experiments; FMA performed confocal and cell death analysis for all RPM1 experiments; SS created RPS5 entry and destination constructs, performed cell death and Western blot analysis for RPM1 and RPS5, and confocal analysis for RPS5.; JK created pADR1::ADR1-YFP and assisted in the co-immunoprecipitation experiments; AB performed some cell death analysis for RNLs; ES, VB and LW assisted in creating RNL and CNL entry and destination constructs; MD generated and characterized SAC1 and dOCRL

constructs; YJ and M-CC provided unpublished SAC1 and dOCRL constructs; SCS, FMA, MTN and FEK conceived the study and designed the experiments; FEK wrote the manuscript with help of SCS and FMA; SCS and FEK edited the revised version of the manuscript with help of CO; SS, AB, YJ, M-CC, JLD and MTN reviewed and edited the manuscript.

ORCID

Marie-Cécile Caillaud https://orcid.org/0000-0002-0348-7024
Jeffery L. Dangl https://orcid.org/0000-0003-3199-8654
Farid El Kasmi https://orcid.org/0000-0002-4634-7689
Yvon Jaillais https://orcid.org/0000-0003-4923-883X
Marc T. Nishimura https://orcid.org/0000-0003-4666-6900
Claudia Oecking https://orcid.org/0000-0003-0635-6457
Svenja C. Saile https://orcid.org/0000-0003-2258-3166
Sruthi Sunil https://orcid.org/0000-0002-2142-5935

Data availability

The data that support the findings of this study are available from the corresponding author upon reasonable request.

References

Ade J, DeYoung BJ, Golstein C, Innes RW. 2007. Indirect activation of a plant nucleotide binding site-leucine-rich repeat protein by a bacterial protease. *Proceedings of the National Academy of Sciences, USA* **104**: 2531–2536.

Andersson MX, Kourtchenko O, Dangl JL, Mackey D, Ellerstrom M. 2006. Phospholipase-dependent signalling during the AvrRpm1- and AvrRpt2-induced disease resistance responses in *Arabidopsis thaliana*. *The Plant Journal* **47**: 947–959.

Balint-Kurti P. 2019. The plant hypersensitive response: concepts, control and consequences. *Molecular Plant Pathology* **20**: 1163–1178.

Bargmann BO, Munnik T. 2006. The role of phospholipase D in plant stress responses. *Current Opinion in Plant Biology* **9**: 515–522.

Bentham AR, Zdrzalek R, De la Concepcion JC, Banfield MJ. 2018. Uncoiling CNLs: structure/function approaches to understanding CC domain function in plant NLRs. *Plant and Cell Physiology* **59**: 2398–2408.

Berkey R, Zhang Y, Ma X, King H, Zhang Q, Wang W, Xiao S. 2017. Homologues of the RPW8 resistance protein are localized to the extrahaustorial membrane that is likely synthesized de novo. *Plant Physiology* **173**: 600–613.

Bi G, Su M, Li N, Liang YU, Dang S, Xu J, Hu M, Wang J, Zou M, Deng Y *et al*. 2021. The ZAR1 resistosome is a calcium-permeable channel triggering plant immune signaling. *Cell* **184**: 3528–3541.

Bonardi V, Tang S, Stallmann A, Roberts M, Cherkis K, Dangl JL. 2011. Expanded functions for a family of plant intracellular immune receptors beyond specific recognition of pathogen effectors. *Proceedings of the National Academy of Sciences, USA* **108**: 16463–16468.

Boyes DC, Nam J, Dangl JL. 1998. The *Arabidopsis thaliana RPM1* disease resistance gene product is a peripheral plasma membrane protein that is degraded coincident with the hypersensitive response. *Proceedings of the National Academy of Sciences, USA* **95**: 15849–15854.

Burdett H, Bentham AR, Williams SJ, Dodds PN, Anderson PA, Banfield MJ, Kobe B. 2019. The plant "resistosome": structural insights into immune signaling. *Cell Host & Microbe* **26**: 193–201.

Castel B, Ngou PM, Cevik V, Redkar A, Kim DS, Yang Y, Ding P, Jones JD. 2019. Diverse NLR immune receptors activate defence via the RPW 8-NLR NRG 1. *New Phytologist* **222**: 966–980.

Chung EH, da Cunha L, Wu AJ, Gao Z, Cherkis K, Afzal AJ, Mackey D, Dangl JL. 2011. Specific threonine phosphorylation of a host target by two unrelated type III effectors activates a host innate immune receptor in plants. *Cell Host & Microbe* **9**: 125–136.

Chung EH, El-Kasmi F, He Y, Loehr A, Dangl JL. 2014. A plant phosphoswitch platform repeatedly targeted by type III effector proteins regulates the output of both tiers of plant immune receptors. *Cell Host & Microbe* **16**: 484–494.

Colin LA, Jaillais Y. 2020. Phospholipids across scales: lipid patterns and plant development. *Current Opinion in Plant Biology* **53**: 1–9.

Collier SM, Hamel LP, Moffett P. 2011. Cell death mediated by the N-terminal domains of a unique and highly conserved class of NB-LRR protein. *Molecular Plant–Microbe Interactions* **24**: 918–931.

Daskalov A, Habenstein B, Sabate R, Berbon M, Martinez D, Chaignepain S, Coulary-Salin B, Hofmann K, Loquet A, Saupe SJ. 2016. Identification of a novel cell death-inducing domain reveals that fungal amyloid-controlled programmed cell death is related to necroptosis. *Proceedings of the National Academy of Sciences, USA* **113**: 2720–2725.

Dondelinger Y, Declercq W, Montessuit S, Roelandt R, Goncalves A, Bruggeman I, Hulpiau P, Weber K, Sehon C, Marquis R *et al*. 2014. MLKL compromises plasma membrane integrity by binding to phosphatidylinositol phosphates. *Cell Reports* **7**: 971–981.

Doumane M, Caillaud MC. 2020. Assessing extrinsic membrane protein dependency to PI4P using a plasma membrane to endosome relocalization transient assay in *Nicotiana benthamiana*. *Methods in Molecular Biology* **2177**: 95–108.

Doumane M, Colin L, Lebecq A, Fangain A, Bareille J, Hamant O, Belkhadir Y, Jaillais Y, Caillaud M-C. 2020. iDePP: a genetically encoded system for the inducible depletion of $PI(4,5)P_2$ in *Arabidopsis thaliana*. *bioRxiv*. doi: 10.1101/2020.05.13.091470.

Duggan C, Moratto E, Savage Z, Hamilton E, Adachi H, Wu C-H, Leary AY, Tumtas Y, Rothery SM, Maqbool A *et al*. 2021. Dynamic localization of a helper NLR at the plant–pathogen interface underpins pathogen recognition. *Proceedings of the National Academy of Sciences, USA* **118**: e2104997118.

El Kasmi F, Chung EH, Anderson RG, Li J, Wan L, Eitas TK, Gao Z, Dangl JL. 2017. Signaling from the plasma-membrane localized plant immune receptor RPM1 requires self-association of the full-length protein. *Proceedings of the National Academy of Sciences, USA* **114**: E7385–E7394.

Engelhardt S, Boevink PC, Armstrong MR, Ramos MB, Hein I, Birch PR. 2012. Relocalization of late blight resistance protein R3a to endosomal compartments is associated with effector recognition and required for the immune response. *Plant Cell* **24**: 5142–5158.

Friedrichsen DM, Joazeiro CA, Li J, Hunter T, Chory J. 2000. Brassinosteroid-insensitive-1 is a ubiquitously expressed leucine-rich repeat receptor serine/threonine kinase. *Plant Physiology* **123**: 1247–1256.

Gao Z, Chung EH, Eitas TK, Dangl JL. 2011. Plant intracellular innate immune receptor resistance to *Pseudomonas syringae* pv. *maculicola* 1 (RPM1) is activated at, and functions on, the plasma membrane. *Proceedings of the National Academy of Sciences, USA* **108**: 7619–7624.

Gronnier J, Crowet J-M, Habenstein B, Nasir MN, Bayle V, Hosy E, Platre MP, Gouguet P, Raffaele S, Martinez D *et al*. 2017. Structural basis for plant plasma membrane protein dynamics and organization into functional nanodomains. *eLife* **6**: e26404.

Heo WD, Inoue T, Park WS, Kim ML, Park BO, Wandless TJ, Meyer T. 2006. PI(3,4,5)P3 and PI(4,5)P2 lipids target proteins with polybasic clusters to the plasma membrane. *Science* **314**: 1458–1461.

Hofmann K. 2020. The evolutionary origins of programmed cell death signaling. *Cold Spring Harbor Perspectives in Biology* **12**: a036442.

Hong Y, Zhao J, Guo L, Kim SC, Deng X, Wang G, Zhang G, Li M, Wang X. 2016. Plant phospholipases D and C and their diverse functions in stress responses. *Progress in Lipid Research* **62**: 55–74.

Hu M, Qi J, Bi G, Zhou JM. 2020. Bacterial effectors induce oligomerization of immune receptor ZAR1 in vivo. *Molecular Plant* **13**: 793–801.

Jacob P, Kim NH, Wu F, El-Kasmi F, Chi Y, Walton WG, Furzer OJ, Lietzan AD, Sunil S, Kempthorn K *et al*. 2021. Plant "helper" immune receptors are Ca(2+)-permeable nonselective cation channels. *Science* **373**: 420–425.

Johansson ON, Fahlberg P, Karimi E, Nilsson AK, Ellerstrom M, Andersson MX. 2014. Redundancy among phospholipase D isoforms in resistance triggered by recognition of the *Pseudomonas syringae* effector AvrRpm1 in *Arabidopsis thaliana*. *Frontiers in Plant Science* **5**: 639.

Jones JD, Dangl JL. 2006. The plant immune system. *Nature* 444: 323–329.

Jubic LM, Saile S, Furzer OJ, El Kasmi F, Dangl JL. 2019. Help wanted: helper NLRs and plant immune responses. *Current Opinion in Plant Biology* 50: 82–94.

Kawano Y, Fujiwara T, Yao A, Housen Y, Hayashi K, Shimamoto K. 2014. Palmitoylation-dependent membrane localization of the rice resistance protein pit is critical for the activation of the small GTPase OsRac1. *Journal of Biological Chemistry* 289: 19079–19088.

Lapin D, Kovacova V, Sun X, Dongus JA, Bhandari D, von Born P, Bautor J, Guarneri N, Rzemieniewski J, Stuttmann J et al. 2019. A coevolved EDS1-SAG101-NRG1 module mediates cell death signaling by TIR-domain immune receptors. *Plant Cell* 31: 2430–2455.

Li J, Wang X. 2019. Phospholipase D and phosphatidic acid in plant immunity. *Plant Science* 279: 45–50.

Li L, Habring A, Wang K, Weigel D. 2020. Atypical resistance protein RPW8/HR triggers oligomerization of the NLR immune receptor RPP7 and autoimmunity. *Cell Host & Microbe* 27: 405–417 e406.

Liu J, Elmore JM, Lin ZJ, Coaker G. 2011. A receptor-like cytoplasmic kinase phosphorylates the host target RIN4, leading to the activation of a plant innate immune receptor. *Cell Host & Microbe* 9: 137–146.

Ma S, Lapin D, Liu LI, Sun Y, Song W, Zhang X, Logemann E, Yu D, Wang J, Jirschitzka J et al. 2020. Direct pathogen-induced assembly of an NLR immune receptor complex to form a holoenzyme. *Science* 370: eabe3069.

Martin R, Qi T, Zhang H, Liu F, King M, Toth C, Nogales E, Staskawicz BJ. 2020. Structure of the activated ROQ1 resistosome directly recognizing the pathogen effector XopQ. *Science* 370: abd9993.

McLaughlin S, Murray D. 2005. Plasma membrane phosphoinositide organization by protein electrostatics. *Nature* 438: 605–611.

Menzel W, Stenzel I, Helbig LM, Krishnamoorthy P, Neumann S, Eschen-Lippold L, Heilmann M, Lee J, Heilmann I. 2019. A PAMP-triggered MAPK cascade inhibits phosphatidylinositol 4,5-bisphosphate production by PIP5K6 in *Arabidopsis thaliana*. *New Phytologist* 224: 833–847.

Monteiro F, Nishimura MT. 2018. Structural, functional, and genomic diversity of plant NLR proteins: an evolved resource for rational engineering of plant immunity. *Annual Review of Phytopathology* 56: 243–267.

Murphy JM. 2020. The killer pseudokinase mixed lineage kinase domain-like protein (MLKL). *Cold Spring Harbor Perspectives in Biology* 12: a036376.

Noack LC, Jaillais Y. 2017. Precision targeting by phosphoinositides: how PIs direct endomembrane trafficking in plants. *Current Opinion in Plant Biology* 40: 22–33.

Platre MP, Noack LC, Doumane M, Bayle V, Simon MLA, Maneta-Peyret L, Fouillen L, Stanislas T, Armengot L, Pejchar P et al. 2018. A combinatorial lipid code shapes the electrostatic landscape of plant endomembranes. *Developmental Cell* 45: 465–480.e11.

Pottinger SE, Innes RW. 2020. RPS5-mediated disease resistance: fundamental insights and translational applications. *Annual Review of Phytopathology* 58: 139–160.

Pruitt RN, Locci F, Wanke F, Zhang L, Saile SC, Joe A, Karelina D, Hua C, Fröhlich K, Wan W-L et al. 2021. The EDS1-PAD4-ADR1 node mediates *Arabidopsis thaliana* pattern-triggered immunity. *Nature*. doi: 10.1038/s41586-021-03829-0.

Qi D, DeYoung BJ, Innes RW. 2012. Structure-function analysis of the coiled-coil and leucine-rich repeat domains of the RPS5 disease resistance protein. *Plant Physiology* 158: 1819–1832.

Qi T, Seong K, Thomazella DPT, Kim JR, Pham J, Seo E, Cho M-J, Schultink A, Staskawicz BJ. 2018. NRG1 functions downstream of EDS1 to regulate TIR-NLR-mediated plant immunity in *Nicotiana benthamiana*. *Proceedings of the National Academy of Sciences, USA* 115: E10979–E10987.

Qin LI, Zhou Z, Li Q, Zhai C, Liu L, Quilichini TD, Gao P, Kessler SA, Jaillais Y, Datla R et al. 2020. Specific recruitment of phosphoinositide species to the plant-pathogen interfacial membrane underlies Arabidopsis susceptibility to fungal infection. *Plant Cell* 32: 1665–1688.

Quarato G, Guy CS, Grace CR, Llambi F, Nourse A, Rodriguez DA, Wakefield R, Frase S, Moldoveanu T, Green DR. 2016. Sequential engagement of distinct MLKL phosphatidylinositol-binding sites executes necroptosis. *Molecular Cell* 61: 589–601.

Rausche J, Stenzel I, Stauder R, Fratini M, Trujillo M, Heilmann I, Rosahl S. 2020. A phosphoinositide 5-phosphatase from *Solanum tuberosum* is activated by PAMP-treatment and may antagonize phosphatidylinositol 4,5-bisphosphate at *Phytophthora infestans* infection sites. *New Phytologist* 229: 469–487.

Reuter L, Schmidt T, Manishankar P, Throm C, Keicher J, Bock A, Oecking C. 2021. Light-triggered and phosphorylation-dependent 14-3-3 association with NONPHOTOTROPIC HYPOCOTYL 3 is required for hypocotyl phototropism. *bioRxiv*. doi: 10.1101/2021.04.09.439179.

Roberts M, Tang S, Stallmann A, Dangl JL, Bonardi V. 2013. Genetic requirements for signaling from an autoactive plant NB-LRR intracellular innate immune receptor. *PLoS Genetics* 9: e1003465.

Saile SC, Jacob P, Castel B, Jubic LM, Salas-Gonzalez I, Backer M, Jones JDG, Dangl JL, El Kasmi F. 2020. Two unequally redundant "helper" immune receptor families mediate *Arabidopsis thaliana* intracellular "sensor" immune receptor functions. *PLoS Biology* 18: e3000783.

Schloffel MA, Salzer A, Wan WL, van Wijk R, Del Corvo R, Semanjski M, Symeonidi E, Slaby P, Kilian J, Macek B et al. 2020. The BIR2/BIR3-associated phospholipase Dγ1 negatively regulates plant immunity. *Plant Physiology* 183: 371–384.

Shimada TL, Betsuyaku S, Inada N, Ebine K, Fujimoto M, Uemura T, Takano Y, Fukuda H, Nakano A, Ueda T. 2019. Enrichment of phosphatidylinositol 4,5-bisphosphate in the extra-invasive hyphal membrane promotes colletotrichum infection of *Arabidopsis thaliana*. *Plant and Cell Physiology* 60: 1514–1524.

Simon ML, Platre MP, Marques-Bueno MM, Armengot L, Stanislas T, Bayle V, Caillaud MC, Jaillais Y. 2016. A PtdIns(4)P-driven electrostatic field controls cell membrane identity and signalling in plants. *Nature Plants* 2: 16089.

Van Ooijen G, Mayr G, Kasiem MMA, Albrecht M, Cornelissen BJC, Takken FLW. 2008. Structure-function analysis of the NB-ARC domain of plant disease resistance proteins. *Journal of Experimental Botany* 59: 1383–1397.

Viotti C, Kruger F, Krebs M, Neubert C, Fink F, Lupanga U, Scheuring D, Boutte Y, Frescatada-Rosa M, Wolfenstetter S et al. 2013. The endoplasmic reticulum is the main membrane source for biogenesis of the lytic vacuole in *Arabidopsis*. *Plant Cell* 25: 3434–3449.

Wang J, Chai J. 2020. Molecular actions of NLR immune receptors in plants and animals. *Science China Life Sciences* 63: 1–14.

Wang J, Chen T, Han M, Qian L, Li J, Wu M, Han T, Cao J, Nagalakshmi U, Rathjen JP et al. 2020a. Plant NLR immune receptor Tm-22 activation requires NB-ARC domain-mediated self-association of CC domain. *PLoS Pathogens* 16: e1008475.

Wang J, Chern M, Chen X. 2020b. Structural dynamics of a plant NLR resistosome: transition from autoinhibition to activation. *Science China Life Sciences* 63: 617–619.

Wang J, Hu M, Wang J, Qi J, Han Z, Wang G, Qi Y, Wang HW, Zhou JM, Chai J. 2019a. Reconstitution and structure of a plant NLR resistosome conferring immunity. *Science* 364: eaav5870.

Wang J, Wang J, Hu M, Wu S, Qi J, Wang G, Han Z, Qi Y, Gao N, Wang HW et al. 2019b. Ligand-triggered allosteric ADP release primes a plant NLR complex. *Science* 364: eaav5868.

Williams SJ, Sornaraj P, deCourcy-Ireland E, Menz RI, Kobe B, Ellis JG, Dodds PN, Anderson PA. 2011. An autoactive mutant of the M flax rust resistance protein has a preference for binding ATP, whereas wild-type M protein binds ADP. *Molecular Plant–Microbe Interactions* 24: 897–906.

Wu Z, Li M, Dong OX, Xia S, Liang W, Bao Y, Wasteneys G, Li X. 2019. Differential regulation of TNL-mediated immune signaling by redundant helper CNLs. *New Phytologist* 222: 938–953.

Wu Z, Tian L, Liu X, Zhang Y, Li X. 2021. TIR signal promotes interactions between lipase-like proteins and ADR1-L1 receptor and ADR1-L1 oligomerization. *Plant Physiology* 187: 681–686.

Xing J, Li X, Wang X, Lv X, Wang L, Zhang L, Zhu Y, Shen Q, Baluska F, Samaj J et al. 2019. Secretion of phospholipase Dδ functions as a regulatory mechanism in plant innate immunity. *Plant Cell* 31: 3015–3032.

Xiong Y, Han Z, Chai J. 2020. Resistosome and inflammasome: platforms mediating innate immunity. *Current Opinion in Plant Biology* 56: 47–55.

Yeung T, Terebiznik M, Yu L, Silvius J, Abidi WM, Philips M, Levine T, Kapus A, Grinstein S. 2006. Receptor activation alters inner surface potential during phagocytosis. *Science* **313**: 347–351.

Yoshioka K, Moeder W, Kang HG, Kachroo P, Masmoudi K, Berkowitz G, Klessig DF. 2006. The chimeric *Arabidopsis* CYCLIC NUCLEOTIDE-GATED ION CHANNEL11/12 activates multiple pathogen resistance responses. *Plant Cell* **18**: 747–763.

Yuan X, Wang Z, Huang J, Xuan H, Gao Z. 2018. Phospholipidase Dδ negatively regulates the function of resistance to *Pseudomonas syringae* pv. *maculicola* 1 (RPM1). *Frontiers in Plant Science* **9**: 1991.

Zhao C, Tang Y, Wang J, Zeng Y, Sun H, Zheng Z, Su R, Schneeberger K, Parker JE, Cui H. 2021. A mis-regulated cyclic nucleotide-gated channel mediates cytosolic calcium elevation and activates immunity in *Arabidopsis*. *New Phytologist* **230**: 1078–1094.

Supporting Information

Additional Supporting Information may be found online in the Supporting Information section at the end of the article.

Fig. S1 Subcellular localization of AtADR1 proteins after transient over-expression in *Nicotiana benthamiana*.

Fig. S2 Subcellular localization of native promoter-driven AtADR1 proteins.

Fig. S3 Characterization of the cell death activity of wild-type (WT), P-loop and QHD variants of AtADR1s.

Fig. S4 AtRPS5 plasma membrane localization and its cell death activity are not affected by MAP-SAC1 or MAP-dOCRL co-expression.

Fig. S5 Degradation of mis-localized AtRPM1 and AtADR1 proteins is not or only partially blocked by proteasome inhibitors.

Fig. S6 Effector-triggered AtRPM1-mediated cell death activity is diminished by PI4P depletion.

Fig. S7 PI4P depletion affects the PM localization of AtADR1 CC_R domains.

Fig. S8 $PI(4,5)P_2$ is not required for the PM localization and stability of AtADR1s and AtRPM1.

Fig. S9 AtADR1s and AtRPM1 cell death activity is not affected by depletion of $PI(4,5)P_2$ from the plasma membrane via MAP-dOCRL co-expression.

Fig. S10 Basic-hydrophobic (BH) profile analysis of CC/CC_R domains.

Fig. S11 Proposed model of AtADR1 localization, oligomerization and function during immunity.

Methods S1 Protocols for the experiments used in this work.

Table S1 Primer list.

Table S2 Transmembrane domain and lipidation prediction summary for *Arabidopsis thaliana* RNLs and the CNLs RPM1 and RPS5.

Please note: Wiley Blackwell are not responsible for the content or functionality of any Supporting Information supplied by the authors. Any queries (other than missing material) should be directed to the *New Phytologist* Central Office.